TABLE IV. The effective cross section for the reaction $\bar{\nu}+e\rightarrow\mu+\bar{\nu}$, defined as the cross section averaged over all the electrons in the Fermi sea that are capable of reacting, is shown as a function of the ratio of the incoming neutrino energy to the threshold neutrino energy.

Neutrino energy / Threshold energy	Effective cross section in cm²
1	0
1.1	1.4×10^{-44}
1.5	1.5×10^{-42}
2	4.4×10^{-41}
3	7.8×10^{-40}
5	1.8×10^{-38}
7	1.3×10^{-37}
10	0.92×10^{-36}

all clear. It is enough to point out here that both of these effects will keep the mean free path finite even where the above simplified analysis implied that it was infinite. The analysis can, however, be considered to give a lower limit to the mean free path.

From these results, we see that neutrino absorption does become very important for high-energy neutrinos in extremely dense matter. Mean free paths of the order of 30 cm for 100-MeV neutrinos for stellar densities of 10^{15} g/cm^3 are to be compared to the characteristic stellar diameter of 10^6 cm. For lower densities, however, or for lower energy neutrinos, it is seen that neutrinos have a remarkably great penetrating ability. Consequently, neutrinos carry energy away from the star with great efficiency.

ACKNOWLEDGMENT

The author would like to acknowledge his deep debt to Professor John A. Wheeler who suggested this project and provided valuable help and encouragement throughout.

PHYSICAL REVIEW VOLUME 133, NUMBER 4B 24 FEBRUARY 1964

Semiphenomenological Solutions of Pion-Nucleon Partial-Wave Dispersion Relations*

A. DONNACHIE AND J. HAMILTON
Department of Physics, University College, Gower Street, London, England

(Received 23 September 1963)

A variational method of solving π-N partial-wave dispersion relations is developed. Analytic trial functions are used, and their parameters are varied to obtain a unitary solution. A good solution for the $(\frac{3}{2},\frac{3}{2})$ resonance is obtained by using the Layson function. The shape of the resonance, as well as its position, is obtained. The only problem about the solution is the validity of the short-range interaction term which is used. Crossing of the real part of the amplitude verifies that it is accurate, but it is not obvious why the variation method should give such a good result. The explanation appears to be that in many cases the low-energy behavior of a partial wave is dominated by the long-range interactions, and a comparatively simple analytic function will give a good solution. An application of the variational method to confirm an earlier analysis of s-wave π-N scattering is also given.

I. INTRODUCTION

WE present a new method for solving partial-wave dispersion relations by using a variational technique. The N/D method[1] which is normally used suffers from certain disadvantages in practice. One disadvantage is that if we have a rough idea of the solution we cannot readily incorporate this information in the N/D method so as to make it easier to get an exact solution. Another disadvantage arises from the fact that the short-range part of the interaction between any pair of elementary particles is unknown (we refer to ranges less than 0.2 10^{-13} cm), and no obvious method exists by which it can be discovered. The ambiguity which this introduces in the N/D method cannot be conveniently handled in practice. Alternatively, we might try to make up for the ignorance about the short-range part of the interaction by imposing high-energy boundary conditions on the partial-wave solutions; for this purpose, some physically reasonable conjectures can be made. However, this approach is again not easy to incorporate in the N/D method. The variational method which is developed here can, to some extent, avoid these various difficulties.

In the variational method, we start with a unitary trial solution $F_p(s)$ which is in practice an algebraic function of s which contains some arbitrary parameters. This trial function is used to approximate the physical integral in the dispersion relation, and thereby give an approximation $\mathrm{Re}F'(s)$ to the real part of the amplitude for physical values of s. Next, the parameters are varied to make $F'(s)$ approach as close to unitarity as possible.

* This work was supported in part by a grant from the Office of Aerospace Research (European Office), U. S. Air Force.

[1] G. F. Chew and S. Mandelstam, Phys. Rev. 119, 467 (1960).

In practice, this is most conveniently done by setting up a second dispersion relation for the imaginary part of the amplitude, so that we have both $\mathrm{Re}F'(s)$ and $\mathrm{Im}F'(s)$ expressed as functions of the parameters. This second dispersion relation is discussed in Sec. II.

The aim of the variational procedure is to make $F'(s)$ unitary, and it turns out that when this has been achieved, $F'(s)$ is also the solution of the dispersion relation. The trial function $F_p(s)$ can be continued through the elastic cut $s_0 \leq s \leq s_2$ on to the unphysical sheet in the usual way. The variational procedure can be looked at in another way. The parameters are varied until the singularities of $F_p(s)$ on the unphysical sheet are consistent (*via* unitarity) with the known singularities on the physical sheet. For example, for a resonance solution, the two resonant poles on the unphysical sheet are adjusted so that, together with the terms representing the interaction, they give the closest possible approach to unitarity on the elastic cut $s_0 \leq s \leq s_2$. The analytic properties on the physical and unphysical sheets and the details of the variational procedure are discussed in Secs. III, IV, and V.

Application of the Method to the $(\frac{3}{2},\frac{3}{2})$ Resonance

The main application of the method is to the $(\frac{3}{2},\frac{3}{2})$ pion-nucleon resonance. From the phenomenological analysis[2] of p-wave pion-nucleon scattering data, it is known that the dominant effect which produces scattering in the π–N $(\frac{3}{2},\frac{3}{2})$ state is the long-range part of the Born term. The next most important effect is the $T=0$ $J=0$ π–π interaction, while the $T=1$ $J=1$ π–π effect and other effects are small.

In our calculation of the low-energy $(\frac{3}{2},\frac{3}{2})$ amplitude, we assume that the spectral function $\rho(s)$ corresponding to these various effects is known. This, of course, means that our calculation is not from first principles. However, there is reason to believe that we could do much better. Starting from the long-range Born term alone (for which it is only necessary to know f^2, the π–N coupling constant), it should be possible to get a rough approximation to the $(\frac{3}{2},\frac{3}{2})$ resonance. Using that, and assuming the $T=0$ $J=0$ π–π phase shifts, it should be possible to get a reasonable approximation to the $T=0$ $J=0$ helicity amplitude for $\pi+\pi\rightarrow N+\bar{N}$. (The small terms, such as the $T=1$ $J=1$ π–π effect, could be estimated in the same way.) Now, an iterative calculation should give a good answer. It would probably be necessary to solve for all the s-wave and p-wave π–N amplitudes together in such an iteration.

Short-Range Term

As we pointed out above, the short-range part of the spectral function $\rho(s)$ is not known. In Sec. VI, we give arguments for believing that a simple pole approximation to this short-range part can be determined by placing certain realistic high-energy boundary conditions on the partial-wave amplitude $F(s)$. That would be of value if the number of parameters in our variational trial function $F_p(s)$ became very large.

In the actual calculations for the $(\frac{3}{2},\frac{3}{2})$ amplitude, which are given in Sec. VII, we use a two-parameter and a three-parameter trial function. These are the Breit-Wigner and Layson forms, respectively. With the Layson form, we obtain a very close approach to unitarity; this is because the Layson form can approximate well to the correct shape of the $(\frac{3}{2},\frac{3}{2})$ resonance, whereas the Breit-Wigner form cannot. In the Layson form, there is a variable width, which allows for the fact that a high-energy p-wave pion is not nearly so much affected by the centrifugal barrier as a low-energy p-wave pion.

With these few-parameter trial functions, the short range part of the spectral function $\rho(s)$ (in the form of a short range pole) is determined by unitarity, and to a small extent by our assumptions about the form and magnitude of the partial wave at energies above 600 MeV. Crossing of the real part of the $(\frac{3}{2},\frac{3}{2})$ partial-wave amplitude provides a good and independent check on the short-range term, and our best solution satisfies this check well.

In Sec. IX, we discuss reasons why our $(\frac{3}{2},\frac{3}{2})$ solutions give such a good estimate of the short-range term. We examine an N/D example in which the short-range and long-range parts of the spectral function are well separated. The example shows that in a large class of problems the short-range part of the spectral function, even if it is very strong, has little effect on the low-energy scattering. In such cases, the long-range interactions dominate the low-energy scattering, and we would expect that a few-parameter trial function $F_p(s)$ which has a few poles on the physical and unphysical sheets, would give a good approximation. This appears to be the reason why we get such good results for the $(\frac{3}{2},\frac{3}{2})$ amplitude.

It should be mentioned that a recent calculation of the $(\frac{3}{2},\frac{3}{2})$ resonance by Singh and Udgaonkar[3] uses a very different approach. These authors try to estimate the short-range term by using a dispersion relation in the momentum transfer t to determine the partial-wave amplitude at the threshold of the crossed physical cut. This is far from easy, and it is not clear that all the short-range contributions to this second dispersion relation have been included.[4]

Purely Phenomenological Application

In Sec. VII, the variational method is applied to a purely phenomenological problem. An analysis[2,5] of the

[2] J. Hamilton, P. Menotti, G. C. Oades, and L. L. J. Vick, Phys. Rev. **128**, 1881 (1962).

[3] V. Singh and B. Udgaonkar, Phys. Rev. **130**, 1177 (1963).

[4] A further comment is that Singh and Udgaonkar neglect the $T=0$ $J=0$ π–π effect, which is quite important.

[5] J. Hamilton, T. D. Spearman, and W. S. Woolcock, Ann. Phys. (N. Y.) **17**, 1 (1962).

low-energy s-wave $\pi-N$ data has shown the role of the $T=0$ $J=0$ π-π interaction, as well as the role of the $T=1$ $J=1$ π-π interaction, in π-N scattering. From this, the $T=0$ s-wave π-π scattering length and the ρ-N coupling constant C_1 can be determined. These results were obtained by fitting the s-wave π-N dispersion relations on the physical cut and on the crossed physical cut. The variational method can be used to obtain the same results by fitting the dispersion relation on the physical cut only. This provides useful confirmation of the phenomenological analysis,[5] and also gives a better determination of C_1.

II. DISPERSION RELATION FOR Im$f(s)$

The pion-nucleon partial-wave amplitude $f(s)$ is defined by

$$f(s)=(e^{2i\delta(s)}-1)/2iq\,, \tag{1}$$

where q is the momentum in the c.m. system and $\delta(s)$ is the phase shift. Also $s=\{(M^2+q^2)^{1/2}+(\mu^2+q^2)^{1/2}\}^2$, where M and μ are the nucleon and pion masses. In the elastic region $(M+\mu)^2\leq s\leq(M+2\mu)^2$, $\delta(s)$ is real. For $(M+2\mu)^2\leq s\leq\infty$, $\delta(s)=\alpha+i\beta$, where α, β are real and $\beta\geq 0$. The singularities of $f(s)$ in the complex s plane follow[6,7] from the Mandelstam representation. They are the physical cut $(M+\mu)^2\leq s\leq\infty$, plus certain unphysical cuts which we do not specify for the moment. For simplicity, we assume that the singularities of the analytic function $f(s)$ are the cuts $-\infty\leq s\leq s_1$ and $s_0\leq s\leq\infty$, where $s_0=(M+\mu)^2$, and s_1 is real, with $s_1<s_0$.

Assuming that no subtraction is needed, $f(s)$ obeys the dispersion relation

$$f(s)=\frac{1}{\pi}\int_{s_0}^{\infty}\frac{\mathrm{Im}f(s')}{s'-s}ds'+\frac{1}{\pi}\int_{-\infty}^{s_1}\frac{\mathrm{Im}f(s')}{s'-s}ds'\,, \tag{2}$$

where in the integrands we write Im$f(s')$ for Im$f(s'+i0)$.

On the physical cut $s_0\leq s\leq\infty$, Eq. (2) gives

$$\mathrm{Re}f(s)=\frac{1}{\pi}P\int_{s_0}^{\infty}\frac{\mathrm{Im}f(s')}{s'-s}ds'+\frac{1}{\pi}\int_{-\infty}^{s_1}\frac{\rho(s')}{s'-s}ds'\,, \tag{3}$$

where we have written $\rho(s')=\mathrm{Im}f(s')$ for $-\infty\leq s'\leq s_1$.

Consider the analytic function

$$g(s)=f(s)/(s-s_0)^{1/2}.$$

Here, $(s-s_0)^{1/2}$ is defined in the plane cut along $s_0\leq s\leq\infty$, so that it has the values $+(s-s_0)^{1/2}$ and $-(s-s_0)^{1/2}$ just above, and just below the cut $s_0\leq s\leq\infty$, where $(s-s_0)^{1/2}$ is the positive root. Then, on $-\infty\leq s\leq s_1$, $(s-s_0)^{1/2}=i(s_0-s)^{1/2}$, where $(s_0-s)^{1/2}$ is the positive root. It follows that the function $g(s)$ has the same cuts as $f(s)$. Further, we have

(i) $g(s)=\dfrac{\mathrm{Re}f(s)+i\,\mathrm{Im}f(s)}{(s-s_0)^{1/2}}$ just above $s_0\leq s\leq\infty$;

(ii) $g(s)=\dfrac{-\mathrm{Re}f(s)+i\,\mathrm{Im}f(s)}{(s-s_0)^{1/2}}$ just below $s_0\leq s\leq\infty$;

(iii) $g(s)=\dfrac{\mathrm{Re}f(s)+i\,\mathrm{Im}f(s)}{i(s_0-s)^{1/2}}$ just above $-\infty\leq s\leq s_1$;

(iv) $g(s)=\dfrac{\mathrm{Re}f(s)-i\,\mathrm{Im}f(s)}{i(s_0-s)^{1/2}}$ just below $-\infty\leq s\leq s_1$.

Cauchy's theorem now gives the dispersion relation for $g(s)$:

$$\frac{f(s)}{(s-s_0)^{1/2}}=\frac{1}{\pi i}\int_{s_0}^{\infty}\frac{\mathrm{Re}f(s')}{(s'-s_0)^{1/2}(s'-s)}ds'+\frac{1}{\pi i}\int_{-\infty}^{s_1}\frac{\mathrm{Im}f(s')}{(s_0-s')^{1/2}(s'-s)}ds'. \tag{4}$$

On the physical cut $s_0\leq s\leq\infty$, Eq. (4) gives[8]

$$\frac{\mathrm{Im}f(s)}{(s-s_0)^{1/2}}=-\frac{1}{\pi}P\int_{s_0}^{\infty}\frac{\mathrm{Re}f(s')}{(s'-s_0)^{1/2}(s'-s)}ds'-\frac{1}{\pi}\int_{-\infty}^{s_1}\frac{\rho(s')}{(s_0-s')^{1/2}(s'-s)}ds'. \tag{5}$$

This relation exists provided relation (3) exists. The dispersion relation (5) is *not* independent of the relation (3). From (3), we obtain the relation (2) for s in the neighborhood of the cut $s_0\leq s\leq\infty$. Now, Eq. (2) can be used to continue $f(s)$ to the neighborhood of the cut $-\infty\leq s\leq s_1$. This shows that $\mathrm{Im}f(s\pm i0)=\pm\rho(s)$ on $-\infty\leq s\leq s_1$. That is sufficient to give Eq. (5). In practice, however, it turns out to be more convenient to use Eqs. (3) and (5) together, rather than Eq. (3) by itself.

III. UNPHYSICAL SHEETS AND UNIQUENESS

The momentum $q(s)$ of the π-N system is defined by[7]

$$[q(s)]^2=\frac{[s-(M+\mu)^2][s-(M-\mu)^2]}{4s}.$$

Thus, $q(s)$ can be defined uniquely on a two-sheeted Riemann surface having branch lines $0\leq s\leq(M-\mu)^2$ and $(M+\mu)^2\leq s\leq\infty$ (Fig. 1). With the notation of Fig. 1,

$$q(s)=\tfrac{1}{2}(r_0r_1/r)^{1/2}\exp[i(\theta_0+\theta_1-\theta)/2]. \tag{6}$$

[6] S. W. MacDowell, Phys. Rev. **116**, 774 (1960).

[7] J. Hamilton and T. D. Spearman, Ann. Phys. (N. Y.) **2**, 172 (1961).

[8] This type of dispersion relation was first used by W. Gilbert, Phys. Rev. **108**, 1078 (1957).

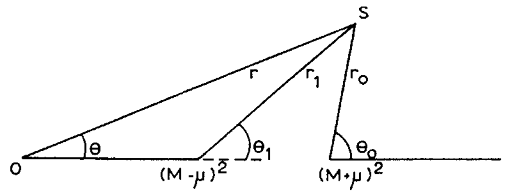

FIG. 1. Location of the branch lines of the c.m. momentum $q(s)$ in the complex s plane and the parameters used in its definition [see Eq. (6)].

Here, $(r_0r_1/r)^{1/2}$ is always real and positive. From Eq. (6), it follows that on the physical sheet

$$q(s\pm i0)=\pm\tfrac{1}{2}(r_0r_1/r)^{1/2},\quad (M+\mu)^2\le s\le\infty;$$
$$q(s\pm i0)=\mp\tfrac{1}{2}(r_0r_1/r)^{1/2},\quad 0\le s\le(M-\mu)^2;$$
$$q(s)=i(r_0r_1/r)^{1/2}/2,\quad -\infty\le s\le 0 \text{ and } (M-\mu)^2\le s\le(M+\mu)^2.$$

Crossing the physical cut $(M+\mu)^2\le s\le\infty$, we get on to the unphysical sheet. On this sheet, all the above values reverse sign. Notice that $q(s^*)=-q^*(s)$ when s and s^* are on the same sheet.

Continued Function $f^{\mathrm{II}}(s)$

The first inelastic threshold in π-N scattering occurs at $s=(M+2\mu)^2$. For convenience, we write $s_2\equiv(M+2\mu)^2$.

A *unitary function* $f^{\mathrm{I}}(s)$ is any analytic function defined on the physical sheet, so that (i) it has the form shown in Eq. (1) where $\delta(s)$ is real just above the elastic cut $s_0=(M+\mu)^2\le s\le s_2$; (ii) it obeys the reality condition $f^{\mathrm{I}}(s^*)=[f^{\mathrm{I}}(s)]^*$. The continuation of a unitary function through the elastic cut is well known[9]; we briefly mention some of the important results.

The continuation across $s_0\le s\le s_2$ is defined by

$$f^{\mathrm{II}}(s)=f^{\mathrm{I}}(s)/[1+2iq(s)f^{\mathrm{I}}(s)],\qquad (7)$$

where $q(s)$ has the physical sheet value. For $s_0\le s\le s_2$, Eq. (1) gives

$$f^{\mathrm{I}}(s+i0)=\frac{e^{i\delta}\sin\delta}{q(s+i0)},\quad (\delta \text{ real})$$

so

$$f^{\mathrm{II}}(s+i0)=\frac{e^{-i\delta}\sin\delta}{q(s+i0)}=\{f^{\mathrm{I}}(s+i0)\}^*=f^{\mathrm{I}}(s-i0).\qquad (8)$$

The last step follows from the reality condition. Equation (8) shows that $f^{\mathrm{II}}(s)$ is the continuation of $f^{\mathrm{I}}(s)$ across $s_0\le s\le s_2$. However, $f^{\mathrm{II}}(s)$ is not the continuation of $f^{\mathrm{I}}(s)$ across the cut $s_2\le s\le\infty$ or across the cut $0\le s\le(M-\mu)^2$. The unphysical sheet reached by continuing through the elastic cut $s_0\le s\le s_2$ will be called the *second sheet.* $f^{\mathrm{II}}(s)$ is the value $f^{\mathrm{I}}(s)$ takes on this sheet.

Inverting Eq. (7) gives

$$f^{\mathrm{I}}(s)=f^{\mathrm{II}}(s)/[1-2iq(s)f^{\mathrm{II}}(s)],\qquad (9)$$

where again $q(s)$ has the physical sheet value. The relation $q(s^*)=-q^*(s)$ and the reality condition for $f^{\mathrm{I}}(s)$ give

$$f^{\mathrm{II}}(s^*)=[f^{\mathrm{II}}(s)]^*.\qquad (10)$$

Let $f^{\mathrm{I}}(s)$ be a π-N partial-wave amplitude. The cuts of $q(s)$ are contained in the cuts[7] of $f^{\mathrm{I}}(s)$, and Eqs. (7) and (9) show that the analytic functions $f^{\mathrm{I}}(s)$ and $f^{\mathrm{II}}(s)$ have the same cuts (although they have different discontinuities across these cuts). By Eq. (10), the discontinuity of $f^{\mathrm{II}}(s)$ across a cut lying along the real axis is $2i\,\mathrm{Im}f^{\mathrm{II}}(s+i0)$.

From Eq. (7) it follows that $f^{\mathrm{II}}(s)$ is regular at any isolated pole of $f^{\mathrm{I}}(s)$. However, it will frequently happen that $f^{\mathrm{II}}(s)$ has a pole[10] near a pole of $f^{\mathrm{I}}(s)$.

If, near $s=s_i$,

$$f^{\mathrm{I}}(s)=A/(s-s_i)+h(s),$$

where $h(s)$ is a slowly varying function of s, then $f^{\mathrm{II}}(s)$ has a pole at

$$s=s_i+A/[(i/2q)-h(s)].$$

If $h(s)$ is not close to $(i/2q)$ and if the residue A is not large, then $f^{\mathrm{II}}(s)$ has a pole near the pole s_i of $f^{\mathrm{I}}(s)$.

Poles of $f^{\mathrm{II}}(s)$ are zeros of the S matrix:

$$S(s)\equiv 1+2iq(s)f^{\mathrm{I}}(s)=e^{2i\delta(s)}.$$

A pole of $f^{\mathrm{II}}(s)$ lying near the physical cut $s_0\le s\le\infty$ gives a resonance, while a pole of $f^{\mathrm{II}}(s)$ on the real axis just to the left of the physical threshold $s_0=(M+\mu)^2$ gives a virtual bound state.

Finally, we compare the discontinuities in $f^{\mathrm{I}}(s)$ and $f^{\mathrm{II}}(s)$ across the cut $-\infty\le s\le 0$. On this cut, $q(s)=i|q(s)|$. If $f(s+i0)-f(s-i0)\equiv 2i\Delta f(s)$, then Eq. (7) gives

$$\frac{\Delta f^{\mathrm{II}}(s)}{\Delta f^{\mathrm{I}}(s)}=\frac{1}{|1-2|q|f^{\mathrm{I}}(s)|^2},\quad (-\infty\le s\le 0).$$

K Functions and Unitarity

We may now examine the problem of the uniqueness of the solution of the partial-wave dispersion relations Eqs. (3) and (5) in the case that the weight function $\rho(s)(-\infty\le s\le s_1)$ is given. In the case that the scattering is purely elastic, the N/D method shows that unitarity implies a unique solution for the amplitude $f(s)$ (apart from the CDD ambiguity[11]). In order to under-

[9] See, for example, R. Oehme, Phys. Rev. **121**, 1840 (1961); W. Zimmermann, Nuovo Cimento **21**, 249 (1961); R. E. Peierls, in *Proceedings of the Conference on Nuclear and Meson Physics, Glasgow, 1954* (Pergamon Press, Inc., New York, 1954), p. 296.

[10] R. Blankenbecler, M. L. Goldberger, S. W. MacDowell, and S. B. Treiman, Phys. Rev. **123**, 692 (1961).

[11] L. Castillejo, R. H. Dalitz, and F. J. Dyson, Phys. Rev. **101**, 453 (1956).

stand the new method of solving partial-wave dispersion relations which is presented below, it is useful to look at the uniqueness problem in another way.

We define a K function to be an analytic function of s such that, (a) its only singularity on the physical sheet is the cut $s_0 \leq s \leq \infty$; (b) it obeys the reality condition $K(s^*) = K^*(s)$. It is easy to write down an example. Let $(s-s_0)_p^{1/2}$ be the value of $(s-s_0)^{1/2}$ on the physical sheet. Thus, $(s-s_0)_p^{1/2} = +(s-s_0)^{1/2}$ when s is just above the cut $s_0 \leq s \leq \infty$. Then,[12]

$$K(s) = \frac{\beta}{s-s_k}\frac{1}{2}\left\{1-\frac{(s-s_0)^{1/2}}{(s_k-s_0)_p^{1/2}}\right\} + \frac{\beta^*}{s-s_k^*}\frac{1}{2}\left\{1-\frac{(s-s_0)^{1/2}}{(s_k^*-s_0)_p^{1/2}}\right\}, \quad (11)$$

where β and s_k are any complex constants, is a K function. Many other varieties of K functions are readily written down.[13]

The importance of K functions lies in the fact that they satisfy the dispersion relations

$$\begin{aligned} \mathrm{Re}K(s) &= \frac{1}{\pi}P\int_{s_0}^{\infty}\frac{\mathrm{Im}K(s')}{s'-s}ds', \\ \frac{\mathrm{Im}K(s)}{(s-s_0)^{1/2}} &= -\frac{1}{\pi}P\int_{s_0}^{\infty}\frac{\mathrm{Re}K(s')}{(s'-s_0)^{1/2}(s'-s)}ds', \end{aligned} \quad (12)$$

provided the integrals converge. Here,

$$\mathrm{Im}K(s') \equiv \mathrm{Im}K(s'+i0).$$

Uniqueness

Now, assume that $\rho(s)$, the discontinuity in a partial-wave amplitude $f(s)$ across the cut $-\infty \leq s \leq s_1$, is given. Suppose $f(s)$ is any solution of the dispersion relations (3) or (5). Then, the function

$$g(s) = f(s) + \textstyle\sum_k K_k(s) \quad (13)$$

is also a solution of Eqs. (3) and (5), provided $K_k(s)$ are any K functions. This is because the functions $K_k(s)$ obey the homogeneous dispersion relations (12).

The functions $K_k(s)$ must have some singularities on an unphysical sheet,[13] apart from the cut $s_0 \leq s \leq \infty$. Thus, the indeterminateness in the solution (13) of Eqs. (3) and (5) is associated with singularities on an unphysical sheet. Requiring that $g(s)$ be unitary on the elastic cut $s_0 \leq s \leq s_2$ makes it possible to continue $g(s)$ across the elastic cut on to the second sheet. This determines the singularities of the K functions on the second sheet and removes the arbitrariness which was associated with them.

[12] Note that $(s^*-s_0)^{1/2} = -\{(s-s_0)^{1/2}\}^*$ when s and s^* are on the same sheet.

[13] We exclude the trivial case $K(s) = \text{const}$.

Of course, there are other unphysical sheets, which are reached by continuing through the cut $s_2 \leq s \leq \infty$. These sheets are associated with inelastic processes, and K functions can have singularities on such sheets. It is a much more difficult problem to remove the ambiguities associated with such singularities.[14] In the applications below, we consider low-energy π–N phenomena for which there is good reason to believe that the indeterminateness due to inelastic processes is unimportant (at least, to the accuracy which can at present be achieved).

It should be noted that we avoid ambiguities of the CDD type[11] caused by $f(s)$ vanishing on $s_0 \leq s \leq \infty$, simply by not choosing solutions of this nature.

IV. VARIATIONAL METHOD

Consider a π–N partial-wave amplitude $f(s)$ which is associated with orbital angular momentum l. It is convenient to use the function

$$F(s) = f(s)/q^{2l}, \quad (14)$$

where $f(s)$ is given by Eq. (1). Near the physical threshold $s_0 = (M+\mu)^2$,

$$\begin{aligned} \mathrm{Re}F(s) &= a + 0(q^2), \\ \mathrm{Im}F(s) &= a^2 q^{2l+1}\{1+0(q^2)\}, \end{aligned} \quad (15)$$

where the constant a is the scattering length. The function $F(s)$ obeys the dispersion relations

$$\begin{aligned} \mathrm{Re}F(s) &= \frac{1}{\pi}P\int_{s_0}^{\infty}\frac{\mathrm{Im}F(s')}{s'-s}ds' + \frac{1}{\pi}\int_{-\infty}^{s_1}\frac{\rho(s')}{s'-s}ds', \\ \frac{\mathrm{Im}F(s)}{(s-s_0)^{1/2}} &= -\frac{1}{\pi}P\int_{s_0}^{\infty}\frac{\mathrm{Re}F(s')}{(s'-s_0)^{1/2}(s'-s)}ds' \\ &\quad -\frac{1}{\pi}\int_{-\infty}^{s_1}\frac{\rho(s')}{(s_0-s')^{1/2}(s'-s)}ds', \end{aligned} \quad (16)$$

for $s_0 \leq s \leq \infty$. The weight function $\rho(s)$ now differs from that appearing in Eqs. (3) and (5) since it contains the kinematic factor $\{q(s)\}^{-2l}$. We assume for the present that $\rho(s)$ is known over the whole range $-\infty \leq s \leq s_1$.

Now we pick a *trial function* $F_p(s)$. It has to be an analytic function which obeys the reality condition $F_p(s^*) = \{F_p(s)\}^*$ and satisfies the unitary condition

$$\mathrm{Im}\{F_p(s)\}^{-1} = -\{q(s)\}^{2l+1} \quad (17)$$

on the elastic cut $s_0 \leq s \leq s_2$. $F_p(s)$ should be a function of a small number of parameters (a_i) and it should be of a form which might reasonably give a tolerable approximation to the exact solution $F(s)$ for physical

[14] For a discussion of the N/D method when inelasticity is important, see G. Frye and R. L. Warnock, Phys. Rev. **130**, 478 (1963).

values of s. For example, if the weight function $\rho(s)$ suggests that a resonance may occur, then the Breit-Wigner form

$$F_p(s)=\Gamma/[(\omega_R-\omega)-i\Gamma q^{2l+1}]$$

could be employed. Here, $\omega=(\mu^2+q^2)^{1/2}$ is the pion energy, and the constants (ω_R,Γ) are the parameters.

The trial function $F_p(s)$ is used to approximate the physical integrals in Eqs. (16). Thus, in effect, we define a new function $F'(s)$ on $s_0\leq s\leq\infty$ by the equations:

$$\mathrm{Re}F'(s)=\frac{1}{\pi}P\int_{s_0}^{\infty}\frac{\mathrm{Im}F_p(s')}{s'-s}ds'+\frac{1}{\pi}\int_{-\infty}^{s_1}\frac{\rho(s')}{s'-s}ds',\quad (s_0\leq s\leq\infty);\quad (18)$$

$$\frac{\mathrm{Im}F'(s)}{(s-s_0)^{1/2}}=-\frac{1}{\pi}P\int_{s_0}^{\infty}\frac{\mathrm{Re}F_p(s')}{(s'-s_0)^{1/2}(s'-s)}ds'-\frac{1}{\pi}\int_{-\infty}^{s_1}\frac{\rho(s')}{(s_0-s')^{1/2}(s'-s)}ds'.$$

In general, $F'(s)$ defined by Eqs. (18) is not a solution of the dispersion relations (16) and, in general, $F'(s)\neq F_p(s)$. [If $F'(s)=F_p(s)$, then $F_p(s)$ is the solution of Eqs. (16).] On the other hand, the analysis in Sec. V below shows that $\mathrm{Re}F'(s)$ and $\mathrm{Im}F'(s)$ are the real and imaginary parts of an analytic function $F'(s)$, which has cuts $-\infty\leq s\leq s_1'$ (where $s_1\leq s_1'\leq s_0$) and $s_0\leq s\leq\infty$, and possibly some isolated poles.

Unitarity Test

The unitary condition is

$$\{\mathrm{Re}F(s)\}^2+\{\mathrm{Im}F(s)\}^2=\mathrm{Im}F(s)/q^{2l+1},\quad (s_0\leq s\leq s_2).\quad (19)$$

The function $F'(s)$ is not in general unitary. The variational procedure consists in varying the parameters (a_i) which occur in $F_p(s)$ to make $F'(s)$ approach unitarity as closely as possible over the elastic cut $s_0\leq s\leq s_2$.

We define

$$D_p(s)=2\frac{\{\mathrm{Re}F'(s)\}^2+\{\mathrm{Im}F'(s)\}^2-\mathrm{Im}F'(s)/q^{2l+1}}{\{\mathrm{Re}F'(s)\}^2+\{\mathrm{Im}F'(s)\}^2+\mathrm{Im}F'(s)/q^{2l+1}}\quad (20a)$$

and

$$\Delta_p^2=\frac{1}{s_2-s_0}\int_{s_0}^{s_2}\{D_p(s)\}^2ds.\quad (20b)$$

Δ_p is the rms deviation of $F'(s)$ from unitarity over the elastic cut. Since $\rho(s)$ is given, Δ_p is only a function of the parameters (a_i). By varying (a_i), we can minimize Δ_p.

If $F'(s)$ is a tolerable approximation to the true solution $F(s)$, we expect that $\mathrm{Im}F'(s)\gtrsim 0$ on the physical cut; and then $|D_p(s)|\lesssim 2$. However, $|D_p(s)|$ has to be very much smaller than this if we are to get a good approximation. The reason is that (as is seen in Sec. V below) we use the properties of $F'(s)$ on the cut $s_0\leq s\leq s_2$ in order to determine the singularities of $F'(s)$ on the second (unphysical) sheet at appreciable distances from this cut. It turns out that an acceptable minimum value of Δ_p is, at the most, about 2%–3%. If Δ_p cannot be brought down to this value, or if a more accurate solution is required, a trial function $F_p(s)$ of different form must be used.

Justification of the Method

By Eq. (17), $F_p(s)$ has a cut $s_0\leq s\leq\infty$. In general, it will also have other cuts and poles on the physical sheet. These lie to the left of the physical cut. For convenience, we express these singularities which are to the left of the physical cut as a number of poles at $s=s_i$ with residues A_i. Thus, $F_p(s)$ obeys the dispersion relations

$$\mathrm{Re}F_p(s)=\frac{1}{\pi}P\int_{s_0}^{\infty}\frac{\mathrm{Im}F_p(s')}{s'-s}ds'+\sum_i\frac{A_i}{s-s_i},$$

$$\frac{\mathrm{Im}F_p(s)}{(s-s_0)^{1/2}}=-\frac{1}{\pi}P\int_{s_0}^{\infty}\frac{\mathrm{Re}F_p(s')}{(s'-s_0)^{1/2}(s'-s)}ds'-\sum_i\frac{A_i}{(s_0-s_i)^{1/2}(s-s_i)},\quad (21)$$

for $s_0\leq s\leq\infty$. Substituting in Eqs. (18) gives

$$\mathrm{Re}F'(s)=\mathrm{Re}F_p(s)-\left\{\sum_i\frac{A_i}{s-s_i}-\sum_j\frac{C_j}{s-s_j}\right\};$$

$$\frac{\mathrm{Im}F'(s)}{(s-s_0)^{1/2}}=\frac{\mathrm{Im}F_p(s)}{(s-s_0)^{1/2}}+\left\{\sum_i\frac{A_i}{(s_0-s_i)^{1/2}(s-s_i)}-\sum_j\frac{C_j}{(s_0-s_j)^{1/2}(s-s_j)}\right\}.\quad (22)$$

In writing Eqs. (22), we have for convenience written those integrals in Eqs. (18) which contain $\rho(s)$ as a sum over a number of poles at $s=s_j$ having residues C_j; i.e., we use $\rho(s)=-\pi\sum_j C_j\delta(s-s_j)$. Since $F_p(s)$ is analytic, it follows from Eqs. (22) that $F'(s)$ is an analytic function.

The numerator of the expression for $D_p(s)$ in Eq. (20a) is

$$Q_p(s)\equiv\{\mathrm{Re}F'(s)\}^2+\{\mathrm{Im}F'(s)\}^2-\mathrm{Im}F'(s)/q^{2l+1}.\quad (23)$$

For $\Delta_p\to 0$, we require $Q_p(s)\to 0$ over the elastic range $s_0\leq s\leq s_2$, since we are dealing with continuous functions of s. Remembering that $F_p(s)$ is unitary, Eqs. (22) give

$$Q_p(s)=-2\,\mathrm{Re}F_p(s)\left\{\sum_i\frac{A_i}{s-s_i}-\sum_j\frac{C_j}{s-s_j}\right\}+2(s-s_0)^{1/2}\left\{\mathrm{Im}F_p(s)-\frac{1}{2q^{2l+1}}\right\}$$
$$\times\left\{\sum_i\frac{A_i}{(s_0-s_i)^{1/2}(s-s_i)}-\sum_j\frac{C_j}{(s_0-s_j)^{1/2}(s-s_j)}\right\}+\left\{\sum_i\frac{A_i}{s-s_i}-\sum_j\frac{C_j}{s-s_j}\right\}^2$$
$$+(s-s_0)\left\{\sum_i\frac{A_i}{(s_0-s_i)^{1/2}(s-s_i)}-\sum_j\frac{C_j}{(s_0-s_j)^{1/2}(s-s_j)}\right\}^2. \quad (24)$$

Suppose that $F_p(s)$ is approximately the same as the true solution $F(s)$ over the physical range $s_0\leq s\leq\infty$. Comparing Eqs. (16) and (21), we see that the last two terms on the right of Eq. (24) are of the second order in small quantities. Further,

$$Q_p(s)=-2\,\mathrm{Re}F(s)\left\{\sum_i\frac{A_i}{s-s_i}-\sum_j\frac{C_j}{s-s_j}\right\}+2(s-s_0)^{1/2}\left[\mathrm{Im}F(s)-\frac{1}{2q^{2l+1}}\right]$$
$$\times\left\{\sum_i\frac{A_i}{(s_0-s_i)^{1/2}(s-s_i)}-\sum_j\frac{C_j}{(s_0-s_j)^{1/2}(s-s_j)}\right\}+\epsilon(s), \quad (25)$$

where $\epsilon(s)$ is of the second order in small quantities.

In general, one or both of the functions $2\,\mathrm{Re}F(s)$ and $2\{\mathrm{Im}F(s)-1/2q^{2l+1}\}$ are large and rapidly varying over the elastic range $s_0\leq s\leq s_2$. Further, the poles s_i and s_j all lie on or near the line $-\infty\leq s\leq s_1$. Thus, in most cases, we expect that the terms in the bracket { } in Eq. (25) are slowly varying functions of s over the elastic range $s_0\leq s\leq s_2$ (the exception is discussed below). Therefore, when we vary the parameters (a_i) to get $\Delta_p\to 0$, this requires

$$\sum_i\frac{A_i}{s-s_i}\to\sum_j\frac{C_j}{s-s_j}$$
$$\sum_i\frac{A_i}{(s_0-s_i)^{1/2}(s-s_i)}\to\sum_j\frac{C_j}{(s_0-s_j)^{1/2}(s-s_j)} \quad (26)$$

for $s_0\leq s\leq s_2$. If $F_p(s)$ is of a suitable form, having sufficient parameters (a_i), the number of poles s_i and s_j can be equal, and Eqs. (26) imply

$$s_i\to s_j;\quad A_i\to C_j. \quad (27)$$

Hence, if we can find a trial function $F_p(s)$ such that Δ_p can be made very small (probably this should be less than 1% in practice), then the singularities of $F_p(s)$ which lie to the left of s_0 on the physical sheet are a good approximation to the analogous singularities of the exact function $F(s)$. As $F'(s)$ is then almost unitary, $F'(s)$ is a good approximation to the solutions of the dispersion relations (16). Of course, in this case, $F'(s)\simeq F_p(s)$ [by Eqs. (22)].

Consistency Test

We now examine the exceptional case which was noted above. In its most general form, this arises when a small minimum value of Δ_p gives a spurious solution. This means that $Q_p(s)$ [Eq. (23)] obeys $Q_p(s)\simeq 0$ for $s_0\leq s\leq s_2$, without (26) being approximately satisfied. Spurious solutions can always be excluded by using Eqs. (22) which show that, for a valid solution, $[F'(s)-F_p(s)]$ must be small on $s_0\leq s\leq\infty$. That is, the *output* $F'(s)$ of Eqs. (18) must differ little from the *input* $F_p(s)$.

This gives us a consistency test. We define[15]

$$\nabla_p^2=\frac{1}{s_2-s_0}\int_{s_0}^{s_2}ds\{\mathrm{Re}F'(s)-\mathrm{Re}F_p(s)\}^2. \quad (28)$$

For a valid solution, it is necessary that $\nabla_p\to 0$ as $\Delta_p\to 0$. This test is used to check our solutions.

Actually, the condition $\nabla_p\to 0$ will by itself give the solution when $\rho(s)$ is known for $-\infty\leq s\leq s_1$. This is because, if $\nabla_p\to 0$, the first of Eqs. (22) leads to the first of relations (26), and this gives (27). However, in practice we use the condition $\Delta_p\to 0$ for three reasons: (a) The rate of convergence towards the true solution should be better if we use both of Eqs. (18) [so that both of Eqs. (26) are involved]. (b) We do not in fact know $\rho(s)$ on the whole of the cut $-\infty\leq s\leq s_1$. The easiest way, in practice, to find the simple pole which replaces the unknown part of $\rho(s)$ involves using both of Eqs. (18). (c) We cannot conveniently choose a trial function which is unitary on $s_0\leq s\leq s_2$ and also gives the correct high-energy behavior.

V. ANALYTIC PROPERTIES OF THE SOLUTION

We have seen that the function $F'(s)$ which is defined for $s_0\leq s\leq s_2$ by Eqs. (18) is analytic, provided $F_p(s)$ is an analytic function. We shall examine further the analytic properties of $F'(s)$. First, we consider the exact solution $F(s)$ defined by Eqs. (14) and (16). Let $F^{\mathrm{I}}(s)$ be its value on the physical sheet and $F^{\mathrm{II}}(s)$ its value on the second sheet obtained by continuation

[15] It may not be necessary to restrict the range to $s_0\leq s\leq s_2$ here.

through the elastic cut $s_0\le s\le s_2$ (cf. Sec. III). By Eqs. (7) and (14),

$$F^{\mathrm{II}}(s)=\frac{F^{\mathrm{I}}(s)}{[1+2i\{q(s)\}^{2l+1}F^{\mathrm{I}}(s)]}, \tag{29}$$

where the physical sheet value of $q(s)$ is used.

From Eq. (29), it follows that on $s_0\le s\le s_2$

$$\mathrm{Re}F(s)=\tfrac{1}{2}\{F^{\mathrm{I}}(s)+F^{\mathrm{II}}(s)\}\equiv R(s)\,,$$

$$\frac{\mathrm{Im}F(s)}{(s-s_0)^{1/2}}=\frac{1}{2i(s-s_0)_p{}^{1/2}}\{F^{\mathrm{I}}(s)-F^{\mathrm{II}}(s)\}\equiv \bar{I}(s)\,, \tag{30}$$

where $\mathrm{Im}F(s)\equiv\mathrm{Im}F(s+i0)$ and $(s-s_0)_p{}^{1/2}$ is the physical sheet value, defined so that it takes the positive value $(s-s_0)^{1/2}$ just above the cut $s_0\le s\le\infty$. The functions $R(s)$ and $\bar{I}(s)$ defined by Eqs. (30) are analytic in the s plane. They are regular and real on the line $s_0\le s\le s_2$; they have cuts $-\infty\le s\le s_1$ and $s_2\le s\le\infty$, as well as poles at the isolated poles of $F^{\mathrm{I}}(s)$ and $F^{\mathrm{II}}(s)$.

Further, $R(s)$ and $\bar{I}(s)$ obey the reality conditions $R(s^*)=R^*(s)$, $\bar{I}(s^*)=\bar{I}^*(s)$. Just above the cut $s_2\le s\le\infty$,

$$F^{\mathrm{I}}(s+i0)=(e^{2i\alpha}e^{-2\beta}-1)/2iq^{2l+1}\,, \tag{31a}$$

where the phase shift is written $\delta=\alpha+i\beta$, α and β being real, and $\beta\ge 0$. By Eq. (29),

$$F^{\mathrm{II}}(s+i0)=(1-e^{-2i\alpha}e^{2\beta})/2iq^{2l+1}\,. \tag{31b}$$

Then, Eqs. (3) give

$$\mathrm{Im}R(s+i0)=\frac{\cos(2\alpha)\sinh(2\beta)}{2q^{2l+1}} \tag{32a}$$

$$s_2\le s\le\infty\,.$$

$$\mathrm{Im}\bar{I}(s+i0)=\frac{\sin(2\alpha)\sinh 2\beta}{2q^{2l+1}} \tag{32b}$$

From these relations, we can express $\mathrm{Re}F(s)$ and $\mathrm{Im}F(s)/(s-s_0)^{1/2}$ for $s_0\le s\le s_2$ in terms of the poles and cuts of $R(s)$ and $\bar{I}(s)$.

This is now done for the unitary trial function $F_p(s)$ which we used in Sec. IV. The result is that, for $s_0\le s\le s_2$,

$$\mathrm{Re}F_p(s)=\tfrac{1}{2}\sum_i\frac{A_i}{s-s_i}+\tfrac{1}{2}\sum_k\frac{B_k}{s-s_k}+\frac{1}{\pi}\int_{s_2}^{\infty}\frac{\mathrm{Im}R_p(s')}{s'-s}ds'\,,$$

$$\frac{\mathrm{Im}F_p(s)}{(s-s_0)^{1/2}}=-\tfrac{1}{2}\sum_i\frac{A_i}{(s-s_i)(s_0-s_i)^{1/2}} \tag{33}$$

$$-\frac{1}{2i}\sum_k\frac{B_k}{(s-s_k)(s_k-s_0)_p{}^{1/2}}+\frac{1}{\pi}\int_{s_2}^{\infty}\frac{\mathrm{Im}\bar{I}_p(s')}{s'-s}ds'\,.$$

Here, for convenience of writing, as in Eqs. (21), we have expressed the physical sheet singularities of $F_p(s)$ which lie to the left of the threshold s_0 as a sum of poles (s_i,A_i). Similarly, a sum of poles (s_k,B_k) is used to represent those singularities of the continued function $F_p{}^{\mathrm{II}}(s)$ which do not lie on the line $s_0\le s\le\infty$. The quantities $\mathrm{Im}R_p(s)$, $\mathrm{Im}\bar{I}_p(s)$ appearing in the last terms in Eqs. (33) are defined in terms of $F_p(s)$ by equations analogous to (32a) and (32b).

Explicit Form of $F'(s)$

Substituting Eqs. (33) in Eqs. (22), we get for $s_0\le s\le s_2$

$$\mathrm{Re}F'(s)=\sum_j\frac{C_j}{s-s_j}-\tfrac{1}{2}\sum_i\frac{A_i}{s-s_i}+\tfrac{1}{2}\sum_k\frac{B_k}{s-s_k}+\frac{1}{\pi}\int_{s_2}^{\infty}\frac{\mathrm{Im}R_p(s')}{s'-s}ds'$$

$$\frac{\mathrm{Im}F'(s)}{(s-s_0)^{1/2}}=-\sum_j\frac{C_j}{(s-s_j)(s_0-s_j)^{1/2}}+\tfrac{1}{2}\sum_i\frac{A_i}{(s-s_i)(s_0-s_i)^{1/2}} \tag{34}$$

$$-\frac{1}{2i}\sum_k\frac{B_k}{(s-s_k)(s_k-s_0)_p{}^{1/2}}+\frac{1}{\pi}\int_{s_2}^{\infty}\frac{\mathrm{Im}\bar{I}_p(s')}{s'-s}ds'.$$

Using

$$F'(s)=\mathrm{Re}F'(s)+i(s-s_0)^{1/2}\{\mathrm{Im}F'(s)/(s-s_0)^{1/2}\}\,, \tag{35}$$

we can now continue the analytic function $F'(s)$ from the line $s_0\le s\le s_2$.

On the physical sheet [obtained by using $(s-s_0)_p{}^{1/2}$ in Eq. (35)], it is seen that $F'(s)$ has poles at $s=s_j$ with residues $2C_j$, and poles at $s=s_i$ with residues $(-A_i)$. In the limit shown in Eq. (27), these poles come together, giving poles at s_j with the correct residues C_j. [Remember that we are using $\rho(s)=-\pi\sum_j C_j\delta(s-s_j)$.] Further, $F'(s)$ has the cut $s_0\le s\le\infty$.

On the second sheet [obtained by using the unphysical sheet value of $(s-s_0)^{1/2}$ in Eq. (35)], we have the analytical continuation of $F'(s)$ through the elastic cut $s_0\le s\le s_2$. This has poles at s_k having residues B_k (and, of course, the cut $s_0\le s\le\infty$).

The last integrals on the right of Eqs. (34) could give large contributions if the parameter β which gives the inelasticity [Eq. (31a)] were to increase too rapidly with s. A similar difficulty has been noted in the N/D method.[14] It appears to be an experimental fact that, for the s- and p-wave π–N amplitudes, inelasticity increases slowly above the inelastic threshold $s_2=(M+2\mu)^2$. In the low-energy s- and p-wave π–N applications below, we assume that the partial-wave amplitudes behave in a specified simple fashion at high energies. Actually, this has the effect that the final integrals in Eqs. (34) give only small and slowly varying contributions for $s_0\le s\le s_2$.

Improved Approximation—The Function $G'(s)$

Using our study of the analytical properties of $F'(s)$, it is easy to see how to improve appreciably a poor variational approximation. If the approximation is poor, some of the physical-sheet singularities (s_i,A_i) of the trial function $F_p(s)$ are a poor approximation to the singularities (s_j,C_j) of the exact solution $F(s)$. We use the function

$$G'(s)=\tfrac{1}{2}\{F'(s)+F_p(s)\}. \tag{36}$$

From Eqs. (33) and (34), we have

$$\mathrm{Re}G'(s)=\tfrac{1}{2}\sum_i \frac{C_j}{s-s_j}+\tfrac{1}{2}\sum_k \frac{B_k}{s-s_k}+\frac{1}{\pi}\int_{s_2}^{\infty}\frac{\mathrm{Im}R_p(s')}{s'-s}ds';$$

$$\frac{\mathrm{Im}G'(s)}{(s-s_0)^{1/2}}=-\tfrac{1}{2}\sum_j \frac{C_j}{(s-s_j)(s_0-s_j)^{1/2}} \tag{37}$$

$$-\frac{1}{2i}\sum_k \frac{B_k}{(s-s_k)(s_k-s_0)_p{}^{1/2}}+\frac{1}{\pi}\int_{s_2}^{\infty}\frac{\mathrm{Im}\bar{I}_p(s')}{s'-s}ds'.$$

Thus, to the left of the threshold s_0, the function $G'(s)$ has the correct singularities (poles at s_j with residues C_j). On the second sheet, $G'(s)$ has poles (s_k,B_k). Applying the variational method to $G'(s)$ determines these unphysical-sheet poles (s_k,B_k). This is done by forming $D_p(s)$ and Δ_p [Eqs. (20a) and (20b)] from $G'(s)$ and minimizing Δ_p.

Because the physical singularities lying to the left of s_0 are correct, and since the variational method now only has to adjust the unphysical-sheet singularities, we expect to get better results by using $G'(s)$ than are obtained by the $F'(s)$ method. In Sec. VIII below, an example is given in which the $G'(s)$ function is a considerable improvement on a poor $F'(s)$ approximation. On the other hand, once a fairly accurate solution $F'(s)$ has been found, there is little point in using the function $G'(s)$.

Systematic Method

The difficulty about the variational methods described above is that it is necessary to use a unitary trial function $F_p(s)$. It may not be easy to find a suitable trial function in any but the simplest cases. We therefore suggest a general variational method which can be applied in a systematic way.

It was pointed out above that, if $F(s)$ is the exact solution, $\mathrm{Re}F(s)$ and $\mathrm{Im}F(s)/(s-s_0)^{1/2}$ can be written in a simple form for $s_0\leq s\leq s_2$. The equations, which are similar to Eqs. (33), are

$$\mathrm{Re}F(s)=\tfrac{1}{2}\sum_j \frac{C_j}{s-s_j}+\tfrac{1}{2}\sum_l \frac{D_l}{s-s_l}+\frac{1}{\pi}\int_{s_2}^{\infty}\frac{\mathrm{Im}R(s')}{s'-s}ds',$$

$$\frac{\mathrm{Im}F(s)}{(s-s_0)^{1/2}}=-\tfrac{1}{2}\sum_j \frac{C_j}{(s-s_j)(s_0-s_j)^{1/2}} \tag{38}$$

$$-\frac{1}{2i}\sum_l \frac{D_l}{(s-s_l)(s_l-s_0)_p{}^{1/2}}+\frac{1}{\pi}\int_{s_2}^{\infty}\frac{\mathrm{Im}\bar{I}(s')}{s'-s}ds',$$

where $s_0\leq s\leq s_2$. Here, as before, (s_j,C_j) are poles which give the physical-sheet singularities lying to the left of the threshold s_0. Also, we assume, as in all the previous sections, that the weight function $\rho(s)$ is known. $\{\rho(s)=-\pi\sum_j C_j\delta(s-s_j)\}$. The second sheet singularities away from the line $s_0\leq s\leq\infty$ are represented, for convenience, by the poles (s_l,D_l). Further, $\mathrm{Im}R(s)$ and $\mathrm{Im}\bar{I}(s)$ are given by Eqs. (32), and we assume that in a low-energy $\pi-N$ problem some empirical or semi-empirical information about the behavior of the partial wave for the higher energies enables us to evaluate the final integrals in Eqs. (38). [We are considering partial waves for which the inelasticity is not important until well above the inelastic threshold $s_2=(M+2\mu)^2$.]

The problem of determining $F(s)$ thus reduces to that of finding the second sheet poles (s_l,D_l). This can be done as follows. Choose a few positions s_l and assign to them arbitrary residues D_l. The properties of the poles and cuts of $f^{\mathrm{II}}(s)$ which were given in Sec. III should help considerably in choosing sensible positions s_l. Now, calculate $\mathrm{Re}F(s)$ and $\mathrm{Im}F(s)(s_0\leq s\leq s_2)$ by Eqs. (38) for these values of (s_l,D_l). Form $D(s)$ and Δ [Eqs. (20a) and (20b)] from these values of $\mathrm{Re}F(s)$ and $\mathrm{Im}F(s)$, and vary s_l and D_l to make Δ minimum. Increasing the number of poles s_l should increase the accuracy of the result. The result can always be checked by substituting it in the original dispersion relation [Eq. (16)].

In the example of the $(\frac{3}{2},\frac{3}{2})$ resonance given below, it was not necessary to use this method, since a very accurate result was obtained using a trial function. In general, however, we expect that this systematic method will be powerful and not too difficult to apply.

VI. HIGH-ENERGY BEHAVIOR AND THE SHORT-RANGE POLE

One of the difficulties which appears when we try to solve the dispersion relations for a $\pi-N$ partial wave $f(s)$ is that we do not have complete knowledge of the spectral function $\rho(s)$ which appears in Eqs. (3) or (5). The positions of the singularities[6,7] of $f(s)$, or of $F(s)$ defined by Eq. (14), are shown in Fig. 2. (The fact that all the singularities do not lie on the real axis gives rise to small, but unimportant, changes in the formulas which were developed in the preceding sections.)

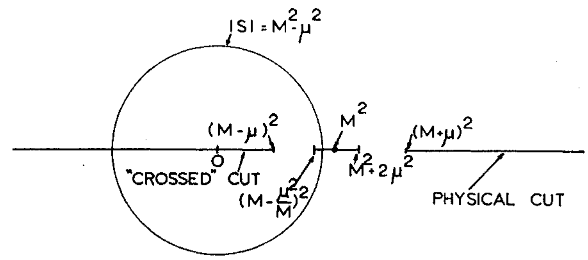

FIG. 2. Location of the singularities of the π–N partial-wave amplitudes in the complex s plane.

It is easy to show[16] how the spectral function $\rho(s)$ can be determined for some of the cuts shown in Fig. 2:

(i) The cut $(M-\mu^2/M)^2 \leq s \leq M^2+2\mu^2$ (and, in the case of the $T=\frac{1}{2}$ $J=\frac{1}{2}$ amplitude, the pole $s=M^2$) gives the long-range part of the Born term. Its contribution is easily calculated, using the coupling constant $f^2 = 0.081$[17,18] (units $\hbar=\mu=c=1$).

(ii) The value of $\rho(s)$ for the cut $0 \leq s \leq (M-\mu)^2$ is evaluated, by crossing, in terms of $\mathrm{Im} f(s)$ for physical values of s. The dominant contributions come from the π–N resonances, and in particular from the $(\frac{3}{2},\frac{3}{2})$ resonance. It may be objected that, in calculating $\rho(s)$ for this cut, we are assuming the results of calculating $f(s)$ from the partial-wave dispersion relations. In fact, more-detailed consideration shows that there is good hope that an iterative calculation will avoid this difficulty. This is especially true when calculating the $(\frac{3}{2},\frac{3}{2})$ amplitude $f_{1+}^{(3/2)}(s)$ itself; because of a factor (1/9) in the p-wave crossing matrix, the contribution of the $(\frac{3}{2},\frac{3}{2})$ resonance to $\rho(s)$ for $0 \leq s \leq (M-\mu)^2$ is unimportant.

(iii) The value of $\rho(s)$ for the arc $0 \leq |\arg s| \leq 66°$ of the circle $|s| = M^2-\mu^2$ is given by the known values[16] of the helicity amplitudes for the process $\pi+\pi \to N+\bar{N}$ for $4 \leq t \leq 50$, where $t=$ (energy)^2 for this process. These values of the helicity amplitudes were determined by a phenomenological analysis[16] of the low-energy s-wave π–N scattering data. These values are used in the calculation of the $(\frac{3}{2},\frac{3}{2})$ amplitude $f_{1+}^{(3/2)}(s)$ in Sec. VIII below. The helicity amplitudes depend on the low-energy π–π scattering phase shifts as well as the low-energy $\pi+N \to \pi+N$ amplitudes. If the low-energy π–π phase shifts only were given, there is some reason to hope that an iterative procedure could be used to give the required helicity amplitudes. However, such a scheme is well beyond the scope of the calculations reported here.

Having determined the spectral functions $\rho(s)$ for the various cuts or parts of cuts in (i), (ii), and (iii) above, it remains that we are ignorant of the value of $\rho(s)$ on the cut $-\infty \leq s \leq 0$, and the portion $66° \leq |\arg s| \leq \pi$ of the circular cut $|s| = M^2-\mu^2$. In order to solve the partial-wave dispersion relations, we have to make some substitute for this lack of knowledge of the short-range part of the π–N interaction.[19] First, we always represent the sum of these short-range parts of the spectral function by using $\rho(s) = -\pi\Gamma\delta(s-\bar{s})$, where $-\infty < \bar{s} < 0$, and Γ is real. That is, the short-range part of $\rho(s)$ is represented by a simple pole $(\bar{s},\Gamma)$ on the negative real axis[20]; we call this the short-range pole. Next, we give as an example an N/D calculation which suggests that we can make up for lack of knowledge of the parameters $\bar{s}$, Γ of the short-range pole by imposing two conditions on the high-energy behavior of the partial-wave amplitude $f_l(s)$.

This provides a possible scheme for solving π–N partial-wave dispersion relations. Realistic high-energy boundary conditions are imposed on the solution $f(s)$; for example, we can assume that the partial wave becomes purely absorptive at infinite energy (i.e., $f(s) \to (i/2q)$ as $q \to \infty$). Then, we try to find short-range pole parameters $\bar{s}$, Γ which, together with the values of $\rho(s)$ calculated as in (i), (ii), (iii) above, give a solution $f(s)$ which satisfies the boundary condition.

N/D Example

Consider an s-wave partial amplitude $f(s)$ which has cuts $-\infty \leq s \leq s_1$ and $s_0 \leq s \leq \infty$. Assume that the discontinuity across the left-hand cut is given by

$$\mathrm{Im} f(s) = \mathrm{Im} f'(s) - \pi\Gamma\delta(s-\bar{s}) \quad (-\infty \leq s \leq s_1), \tag{39a}$$

where

$$\mathrm{Im} f'(s) = 0 \text{ for } -\infty \leq s \leq s_3, \quad (s_3 < s_1). \tag{39b}$$

Also, Γ and $\bar{s}$ are real and $\bar{s} < s_3$. Further, we assume that $q^2 = s - s_0$.

The N and D equations (with a subtraction in the latter) are

$$N(s) = \frac{1}{\pi}\int_{-\infty}^{s_1} \frac{D(s')\,\mathrm{Im} f(s')}{s'-s} ds', \tag{40a}$$

$$D(s) = D(s_0) - \frac{s-s_0}{\pi}\int_{s_0}^{\infty} \frac{N(s')R(s')q'}{(s'-s_0)(s'-s)} ds', \tag{40b}$$

where $R(s) = \{\sigma_{\mathrm{total}}/\sigma_{\mathrm{elastic}}\}$. On substituting Eqs. (39) in Eqs. (4), we can write

$$N(s) = N'(s) + \Gamma\bar{D}/(s-\bar{s}), \tag{41a}$$

where we put $\bar{D} \equiv D(\bar{s})$, and

$$N'(s) = \frac{1}{\pi}\int_{-\infty}^{s_1} \frac{D(s')\,\mathrm{Im} f'(s')}{s'-s} ds'. \tag{41b}$$

Also,

$$D(s) = D(s_0) - \frac{s-s_0}{\pi}\int_{s_0}^{\infty} \frac{N'(s')R(s')q'}{(s'-s_0)(s'-s)} ds' - \frac{s-s_0}{\pi}\int_{s_0}^{\infty} \frac{\Gamma\bar{D}R(s')}{(s'-\bar{s})(s'-s_0)(s'-s)} ds'. \tag{42}$$

For simplicity in calculating the last term in Eq. (42), we write $R(s') = R$ where R is a constant $(1 \leq R \leq 2)$.

[16] See J. Hamilton, T. D. Spearman, and W. S. Woolcock, Ann. Phys. (N. Y.) **17**, 1 (1962); J. Hamilton, P. Menotti, G. C. Oades, and L. L. J. Vick, Phys. Rev. **128**, 1881 (1962) for the details. These papers are referred to as HSW and HMOV, respectively.

[17] W. S. Woolcock, *Proceedings of the International Conference on High Energy Physics, Aix-en-Provence, 1961* (Centre d'Etudes Nucleaires de Saclay, Seine et Oise, 1961), Vol. 1, p. 459.

[18] J. Hamilton and W. S. Woolcock, Rev. Mod. Phys. **35**, 737 (1963).

[19] The values of s for which $\rho(s)$ is unknown correspond roughly to forces of range $\leq \hbar/Mc = 0.210^{-13}$ cm.

[20] It may of course turn out that a single pole does not adequately represent the short-range effects. For the present, we assume that it is sufficient.

Then,

$$D(s)=\begin{cases} D'(s)+\dfrac{\Gamma\bar{D}R}{s-\bar{s}}\left\{\dfrac{s-s_0}{(s_0-\bar{s})^{1/2}}-i(s-s_0)^{1/2}\right\}, & s>s_0 \quad (43a)\\ D'(s)+\dfrac{\Gamma\bar{D}R}{s-\bar{s}}\left\{\dfrac{s-s_0}{(s_0-\bar{s})^{1/2}}+(s_0-s)^{1/2}\right\}, & s<s_0, \quad (43b)\end{cases}$$

where

$$D'(s)=D(s_0)-\frac{s-s_0}{\pi}\int_{s_0}^{\infty}\frac{N'(s')R(s')q'}{(s'-s_0)(s'-s)}ds'. \quad (43c)$$

It is tempting to think that $N'(s)$ and $D'(s)$ provide the solution to the partial-wave problem for which

$$\mathrm{Im}f(s)=\mathrm{Im}f'(s) \quad (-\infty\leq s\leq s_1).$$

That is not the case, because it would require that $D(s')$ be replaced by $D'(s')$ in the integral in Eq. (41b). In fact, $N'(s)$ and $D'(s)$ both depend on $\bar{s}$ and Γ.

However, there are many cases for which this dependence is not strong. Putting $s=\bar{s}$ in Eq. (43b) gives

$$\bar{D}=D'(\bar{s})/[1-\Gamma R/2(s_0-\bar{s})^{1/2}]. \quad (43d)$$

Suppose that the important values of the spectral function $\mathrm{Im}f'(s)$ occur for values of s such that

$$\left|\frac{\Gamma(s_0-s)^{1/2}}{s-\bar{s}}\Big/\left\{1-\frac{\Gamma R}{2(s_0-\bar{s})^{1/2}}\right\}\right|\ll 1;$$

then, it follows from Eq. (43b) that we could replace $D(s')$ by $D'(s')$ in Eq. (41b) without producing a large error. This means that $N'(s)$ and $D'(s)$ do not depend strongly on $\bar{s}$ and Γ. Such a situation occurs if the scattering is dominated by a strong long-range interaction.

If $N'(s)$ and $D'(s)$ do not depend strongly on $\bar{s}$ and Γ, the results which follow are easy to interpret. If they do depend strong on $\bar{s}$ or Γ, the results are still valid, but they cannot be used so readily. Now, let s become very large in Eqs. (41b) and (43c). Then, as $s\to\infty$,

$$\begin{aligned} N'(s)&\to\frac{N'}{s}+\frac{N''}{s^2}+\cdots,\\ \mathrm{Re}D'(s)&\to D'+\frac{D''}{s}+\cdots. \end{aligned} \quad (44)$$

[This statement about $\mathrm{Re}D'(s)$ is true because the integral which gives $\mathrm{Re}D'(s)$ has essentially the same form as the last integral in Eq. (42).] Thus, for large s,

$$f(s)=\frac{(N'+\Gamma\bar{D})+\frac{1}{s}(N''-\bar{s}N')+0(1/s^2)}{\left\{s'\left(D'+\frac{\Gamma\bar{D}R}{(s_0-\bar{s})^{1/2}}\right)+\left(D''-\bar{s}D'-s_0\frac{\Gamma\bar{D}R}{(s_0-\bar{s})^{1/2}}\right)+0\left(\frac{1}{s}\right)\right\}-iq\left\{R\left(N'+\Gamma\bar{D}+\frac{N''}{s}\right)+0\left(\frac{1}{s^2}\right)\right\}}. \quad (45)$$

Conditions on $f(s)$ as $s\to\infty$

Suppose that we impose the boundary condition

$$\frac{\mathrm{Re}f(s)}{\mathrm{Im}f(s)}\to 0 \quad \text{as} \quad s\to\infty. \quad (46a)$$

This requires

$$D'+\Gamma\bar{D}R/(s_0-\bar{s})^{1/2}=0.$$

Using Eq. (43d), this constraint can be written

$$\frac{\Gamma}{(s_0-\bar{s})^{1/2}}=\frac{1}{R}\frac{D'}{\frac{1}{2}D'-D'(\bar{s})}. \quad (46b)$$

When Eq. (46b) holds, Eq. (45) gives

$$f(s)=\frac{i}{qR}\left\{1+0\left(\frac{1}{q}\right)\right\} \quad \text{as} \quad q\to\infty. \quad (46c)$$

So far, as we have required only that $\mathrm{Re}f(s)=0(1/s)$ as $s\to\infty$. Suppose that we impose the second boundary condition,

$$\mathrm{Re}f(s)\to\frac{A}{q^2}, \quad \text{as} \quad q\to\infty, \quad (47a)$$

where the constant A is given. Then, using Eq. (45), we get

$$\{(s_0-\bar{s})+\alpha R(s_0-\bar{s})^{1/2}\}D'=\alpha R^2N'-D''. \quad (47b)$$

Clearly, the two boundary conditions Eqs. (46a) and (47a) which we have imposed on $f(s)$ give two equations [(46b) and (47b)] for $\bar{s}$ and Γ, the parameters of the short-range pole. If these equations have real solutions, they determine the short-range pole. In the application of the variational method, which is given in Sec. VIII below, we use the boundary conditions (46a) and (47a), with $A=0$. This corresponds to purely absorptive high-energy behavior. The example that we have just given suggests that, however many parameters that we introduce into the variational procedure, we will get a unique answer for the parameters $\bar{s}$, Γ of the short-range pole (if any answer exists).

VII. APPLICATION TO THE PHENOMENOLOGICAL ANALYSIS OF s-WAVE π-N SCATTERING

We make this application in order to get a good determination of the coupling constant between the ρ isobar and the nucleon. It is useful to describe it here since it illustrates some of the steps in the variational method.

The phenomenological analysis[16] of the s-wave π–N scattering data showed that the dominant causes of low-energy s-wave scattering (i.e., up to about 200 MeV lab energy) are:

(a) A strong short-range repulsion which was almost the same in the $T=\frac{1}{2}$ and $T=\frac{3}{2}$ isospin states. In units $\hbar=\mu=c=1$, it contributes around -0.3 to the scattering lengths. The scattering lengths are[18] $a_1=0.171 \pm 0.005$, $a_3=-0.088\pm 0.004$.

(b) A fairly strong attraction produced by the low-energy $T=0$ $J=0$ π–π attraction. This contributes equally to the $T=\frac{1}{2}$ and $T=\frac{3}{2}$ π–N s-wave states. It is of comparatively long range, and its effect falls off quickly with increasing energy in the π–N system.

(c) The ρ-exchange effect, which gives an attraction in the $T=\frac{1}{2}$ π–N s wave and a repulsion (of half the magnitude) in the $T=\frac{3}{2}$ s wave. Because of the large mass of the ρ isobar, these contributions to the s-wave π–N amplitudes fall off very little in the energy range 0–200 MeV.

These effects were isolated by fitting the dispersion relation (3) to the data on the low-energy physical region $(M+\mu)^2\leq s\leq 80$ and on the left-hand portion $20\leq s\leq (M-\mu)^2$ of the crossed cut (cf. Fig. 2). In the latter case, crossing symmetry was employed to find $\mathrm{Re}f(s)$ and $\mathrm{Im}f(s)$.

With a narrow-resonance approximation for the ρ isobar, its effect on π–N scattering is given by the position of the isobar $t_R=M_\rho^2$, and the ρ–N coupling constant C_1.[21] Using the experimental value of M_p, the constant C_1 is deduced from the analysis of the π–N s-wave data. Because the separation of the effects (a), (b), and (c) was carried out in a very simple fashion, this determination of C_1 was not precise. The variational method can give a great improvement here.

Details of the Variational Method

We fit the partial-wave dispersion relations to the s-wave π–N data on the elastic region, $s_0=(M+\mu)^2 \leq s\leq (M+2\mu)^2=s_2$. Dispersion relations (18) are used for $F^{(1/2)}(s)$ and $F^{(3/2)}(s)$, the s-wave π–N amplitudes. In Eqs. (18) instead of a trial function $F_p(s)$, we use the actual π–N s-wave scattering data.

Up to 450 MeV, the data used are those described by HMOV.[16] Above 2 BeV, we assume that

$$\mathrm{Re}F^{(T)}(s)=0,\quad \mathrm{Im}F^{(T)}(s)=\frac{1}{2q}\quad (T=\tfrac{1}{2},\tfrac{3}{2}).\tag{48}$$

[21] For the definition of C_1, see Sec. 4 of HMOV (Ref. 16).

This corresponds to totally inelastic partial waves. In the intermediate region, smooth curves are used for $\mathrm{Im}F^{(T)}(s)$ and $\mathrm{Re}F^{(T)}(s)$; these are adjusted so as to join smoothly on to the values in the two other energy regions. As the physical integrals in Eqs. (18) are evaluated only for $s_0\leq s\leq s_2$, any errors due to the approximations that we have made above 450 MeV will be unimportant. This is because the errors will vary little with s, and will be automatically absorbed in the short-range term.

The weight function $\rho(s)$ is calculated in the way that we indicated in paragraphs (i), (ii), and (iii) of Sec. VI. In addition, the short-range pole is given by

$$\rho(s)=-\pi\Gamma\delta(s-\bar{s}),\tag{49}$$

where $-\infty\leq\bar{s}\leq 0$. Γ and $\bar{s}$ will be determined by the variation process when we make the output $F'(s)$ of Eqs. (18) unitary. The π–π terms (Sec. VI, §3) are now described in some more detail.

$T=0$ and $T=1$ π–π Terms

We have to determine the contribution from the $T=0$ and $T=1$ processes $\pi+\pi\to N+\bar{N}$ to the discontinuities of $F^{(1/2)}(s)$ and $F^{(3/2)}(s)$ across the arc $0\leq|\arg s|\leq 66°$ of the circle $|s|=M^2-\mu^2$ (cf. Fig. 2). The $T=0$ $\pi+\pi\to N+\bar{N}$ gives the long-range effect described under (b) above. The analysis of HMOV[16] shows that this is almost entirely due to the $T=0$ $J=0$ state of $\pi+\pi\to N+\bar{N}$. The $T=0$ $J\geq 2$ states appear to give at most a small contribution[16] to the arc $0\leq|\arg s|\leq 66°$ of the circle.

For ease of calculation, the helicity amplitude[22] $f_+^0(t)$ for the $T=0$ $J=0$ process $\pi+\pi\to N+\bar{N}$ is represented in the range $t\geq 4$ by a δ function[23]

$$\mathrm{Im}f_+^0(t)=C_0\delta(t-t_R').\tag{50}$$

This gives the discontinuities in the invariant functions $A^{(+)}(s,t)$, $B^{(+)}(s,t)$ across the circle.

$$\mathrm{Im}A^{(+)}(s,t)=\frac{4\pi}{M^2-t/4}C_0\delta(t-t_R')$$
$$\mathrm{Im}B^{(+)}(s,t)=0.\tag{51}$$

Next, the contribution to the s-wave π–N amplitude $F^{(+)}(s)$ $\{F^{(+)}=\frac{1}{3}F^{(1/2)}+\frac{2}{3}F^{(3/2)}\}$ is found in the usual way.

The parameter t_R' is chosen, once and for all, to give good agreement with the exact energy dependence of the $T=0$ $J=0$ π–π contribution to the s-wave π–N amplitudes from threshold up to 250 MeV, as calculated by HMOV.[16] For this purpose, we use the HMOV calculation with $\nu_1=-30$, $\Gamma=15$ (i.e., π–π, $T=0$ $J=0$

[22] For the notation see HSW (Ref. 16).

[23] This does not mean that the $T=0$ $J=0$ π–π state has a resonance at t_R'. In fact, the analysis of HMOV shows that such a resonance does not fit the low-energy s-wave π–N data when we solve the Omnès equation to get from $\pi+\pi\to\pi+\pi$ to $\pi+\pi\to N+\bar{N}$.

scattering length $a_0=1.3$) [cf. Sec. 3 (vii) of HMOV (Ref. 16)]. This gives $t_R'=10$. It is seen in Fig. 3 that the agreement in the physical region up to 250 MeV is good.

The value of the parameter C_0 is normalized to be unity for the curve shown in Fig. 3. In order to check that the separation of the $T=0$ $J=0$ π–π contribution [i.e., (b) above] in the phenomenological analysis is accurate, the parameter C_0 is included among those to be varied.

The effect of the $T=1$ $J=1$ π–π interaction (ρ) is also described by a δ-function approximation to the helicity amplitudes $\mathrm{Im}f_{\pm}^1(t)$. Analogous to Eqs. (51), this gives

$$\begin{aligned}\mathrm{Im}A_{\pi\pi}^{(-)}(s,t)&=12C_2(s+\tfrac{1}{2}t_R-M^2-\mu^2)\delta(t-t_R)\,,\\ \mathrm{Im}B_{\pi\pi}^{(-)}(s,t)&=-12(C_1+2MC_2)\delta(t-t_R)\,,\end{aligned}\qquad(52)$$

where $t_R=28$ (i.e., $M_\rho=740$ MeV). We take $C_2/C_1=0.27$, as required by the anomalous magnetic moments of the proton and neutron. The contribution to the s-wave π–N amplitudes, coming from the arc $0\leq|\arg s|\leq 66°$, is then calculated[24] with C_1 as a variable parameter. (The phenomenological analysis[16] gave $C_1\approx -1.0$ for $t_R=28$. It should be noted that this is an absolute, not a normalized, value.)

Results for the $T=\frac{1}{2}$ $\pi-N$ s-Wave

Now Eqs. (18) are used to compute $\mathrm{Re}F'(s)$ and $\mathrm{Im}F'(s)$ for $s_0\leq s\leq s_2$. The π–π parameters C_0 and C_1 are given a set of values in the ranges $0.75\leq C_0\leq 1.25$, $-1.25\leq C_1\leq -0.75$. This gives (for $T=\frac{1}{2}$)

$$\mathrm{Re}F'(s)=L(s;C_0,C_1)+\frac{\Gamma}{s-\bar{s}}\,,\qquad(53\text{a})$$

$$\frac{\mathrm{Im}F'(s)}{(s-s_0)^{1/2}}=M(s;C_0,C_1)-\frac{\Gamma}{(s-\bar{s})(s_0-\bar{s})^{1/2}}\,.\qquad(53\text{b})$$

Here, the short-range pole terms [coming from Eq. (49)] are written explicitly. $L(s;C_0,C_1)$ and $M(s;C_0,C_1)$ are now known functions of s, C_0, C_1.

The position $\bar{s}$ of the short-range pole is varied along the axis $-\infty\leq\bar{s}\leq 0$, starting from the origin. For any value of $\bar{s}$, the value of Γ is determined by requiring that $F'(s)$ be unitary at some position s'' in the elastic range[25] ($s_0\leq s''\leq s_2$). In practice, we choose $s''=68$ (i.e., 87.5 MeV lab pion energy). That is, we impose the condition

$$\{\mathrm{Re}F'(s'')\}^2+\{\mathrm{Im}F'(s'')\}^2=\frac{1}{q(s'')}\,\mathrm{Im}F'(s'')\,.\qquad(54)$$

For each set of values of C_0, C_1, $\bar{s}$, this gives a quadratic equation for Γ. Let the roots be Γ_1 and Γ_2. If these roots are not real, then the single-pole approximation for the short-range part [Eq. (49)] is not adequate, and two or more short-range poles have to be used. In the $T=\frac{1}{2}$ s-wave case, the roots Γ_1 and Γ_2 are real.

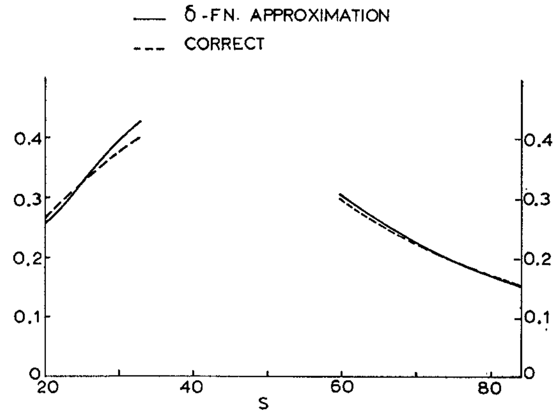

FIG. 3. Comparison of the $T=0$ $J=0$ π–π contribution to s-wave π–N scattering in the δ-function approximation and in the effective-range approximation (Ref. 16) (denoted by "correct").

For each root Γ_i ($i=1, 2$), we form the function $D_i(s)$ defined by Eqs. (20a), and evaluate [cf. Eq. (20b)],

$$[\Delta(\bar{s},\Gamma_i;C_0,C_1)]^2=\frac{1}{s_2-s_0}\int_{s_0}^{s_2}[D_i(s)]^2ds\,.\qquad(55)$$

$\Delta(\bar{s},\Gamma_i;C_0,C_1)$ is the root-mean-square deviation from unitarity over the elastic range $s_0\leq s\leq s_2$. In the $T=\frac{1}{2}$ case, it is found consistently that the value of Δ for one of the two roots Γ_i ($i=1, 2$) is much larger than the value for the other root. The former value can be discarded unambiguously. We can now write $\Delta=\Delta(\bar{s},C_0,C_1)$ for the remaining solution. A typical variation of the residue Γ with the pole position $\bar{s}$ for this solution is shown in Fig. 4.

For fixed C_0, C_1 (in the ranges indicated above), Δ initially decreases as $\bar{s}$ moves to the left from the origin,

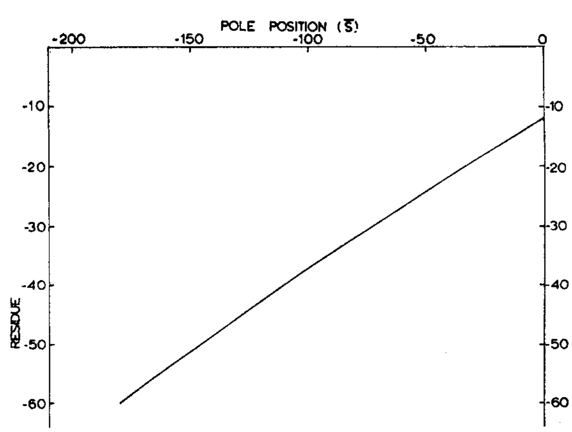

FIG. 4. Typical variation of the residue with position for the short-range pole in the $T=\frac{1}{2}$ π–N s-wave calculation.

[24] For the details, see HMOV (Ref. 16).
[25] Note that $s_0=(M+\mu)^2=59.6$, $s_2=(M+2\mu)^2=76.0$.

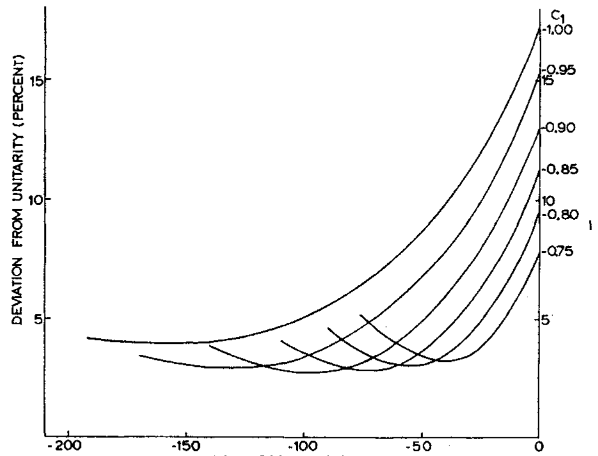

FIG. 5. Variation of the rms deviation from unitarity with position of the short-range pole in the $T=\frac{1}{2}$ π–N s-wave calculation for different values of the parameter C_1, the parameter C_0 being fixed at $C_0=1.00$.

reaches a minimum, and then increases. We denote this minimum value of Δ by $\Delta(C_0,C_1)$, and the corresponding value of $\bar{s}$ by $\bar{s}(C_0,C_1)$. Figures 5 and 6 show examples of this behavior.

Contour Plot

Varying C_1 and keeping C_0 fixed, it is found that the values of $\Delta(C_0,C_1)$ lie on a curve which has a minimum for some value $C_1(C_0)$ of C_1. Figure 5 shows this behavior for the case $C_0=1.00$. Similarly, varying C_0 and keeping C_1 fixed, $\Delta(C_0,C_1)$ lies on a curve which has a minimum for some value $C_0(C_1)$ of C_0. Figure 6 shows this behavior for the case $C_1=-0.95$. A simple way of representing these results is the contour plot of $\Delta(C_0,C_1)$, which is shown in Fig. 7.

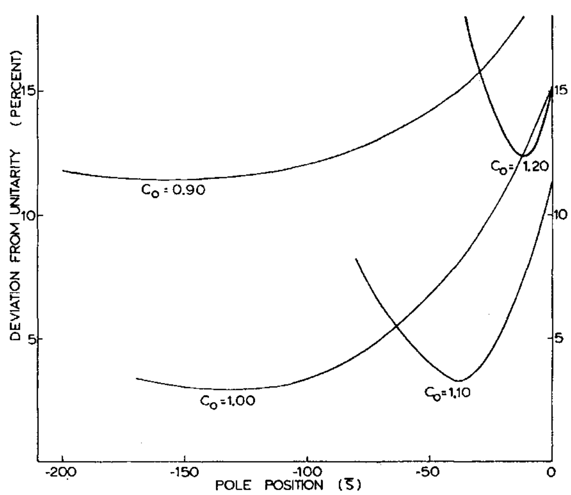

FIG. 6. Variation of the rms deviation from unitarity with position of the short-range pole in the $T=\frac{1}{2}$ π–N s-wave calculation for different values of the parameter C_0, the parameter C_1 being fixed at $C_1=-0.95$.

The lowest point in the contour plot is $\Delta=2.60\%$, which occurs at $C_0=1.025$, $C_1=-0.94$. The corresponding short-range pole $\Gamma/(s-\bar{s})$ has parameters $\bar{s}=-125$, $\Gamma=-42.5$. The short-range pole contributes -0.23 to the $T=\frac{1}{2}$ scattering length a_1.

Figure 8 shows the phase shift α_1 which is obtained from the solution $F'(s)$ having these values of the parameters [we use $\mathrm{Re}F'(s)=(\sin 2\alpha_1)/2q$]. Clearly, this phase shift is very close to the input phase shift, so the solution is self-consistent.

Errors

We assume that the input low-energy π–N phase-shift data are accurate. As was noted above, errors arising from the input data above 450 MeV should be unimportant. We shall attempt to estimate the errors in the values of C_0, C_1 due to the variational method itself.

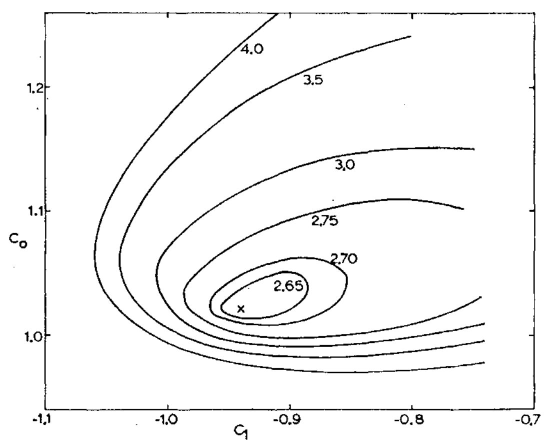

FIG. 7. Contour plot of the percentage rms deviation from unitarity [$\Delta(C_0,C_1)$] as a function of C_0 and C_1 in the $T=\frac{1}{2}\pi$–N s-wave calculation.

Figure 8 shows the band of values of α_1, which is given by $\mathrm{Re}F'(s)=(\sin 2\alpha_1)/2q$ for the values of (C_0,C_1) lying on the contour $\Delta(C_0,C_1)=2.65\%$. The corresponding ranges of the parameters are $1.014<C_0<1.050$, $-0.955<C_1<-0.885$. The best unitary solution for α_1 (corresponding to $C_0=1.025$, $C_1=-0.94$) does not coincide exactly with the input values of α_1, but lies within a band which is about one-quarter of the width of the $\Delta=2.65\%$ band. From this, we deduce that

$$C_0=1.025\begin{matrix}+0.006\\-0.003\end{matrix},\quad C_1=-0.94\pm0.01. \qquad (56)$$

Conclusions

These results are in good agreement with the results of the earlier phenomenological analysis.[16] That gave $C_0=1.00$, $C_1=-0.95$. The present results, obtained by a very different method, provide a useful confirmation of the earlier phenomenological analysis[16] in which the

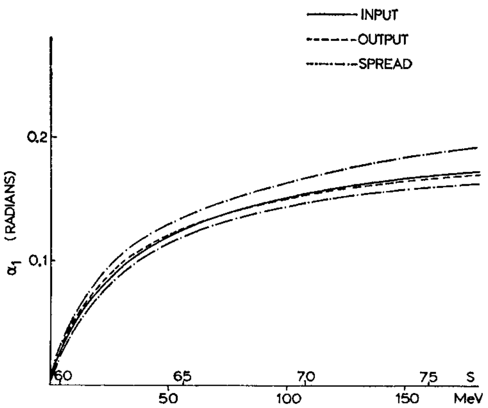

FIG. 8. Comparison of the output $T=\frac{1}{2}$ π–N s-wave phase shift α_1 and error spread with the input.

dispersion relation (3) was fitted on the physical and the crossed cuts. They give considerable support, both qualitative and quantitative, for the conclusions of HMOV[16] on the role of the low-energy π–π interactions in low-energy s-wave π–N scattering.

Results for the $T=\frac{3}{2}$ π–N s-Wave

The analysis was carried out in the same way as for the $T=\frac{1}{2}$ case. The results provide interesting examples of the difficulties which can arise in the variational method.

Again, the ranges $0.75\leq C_0\leq 1.25$, $-1.25\leq C_1\leq -0.75$ were used. For some positions of these ranges of values of C_0 and C_1, the discriminant of the quadratic equation (54) is negative, so that no solution having a single short-range pole exists. For values C_0, C_1 such that the solution does exist, the minima of $\Delta(\bar{s},C_0,C_1)$ as a function of $\bar{s}$ are shallow, as is seen in Figs. 9 and 10. The corresponding value of Γ varies slowly with $\bar{s}$.

The absolute minimum of $\Delta(C_0,C_1)$ is not well-determined in the $T=\frac{3}{2}$ case (cf. Figs. 9 and 10). The values of C_0 and C_1 obtained in the $T=\frac{1}{2}$ case [Eq.

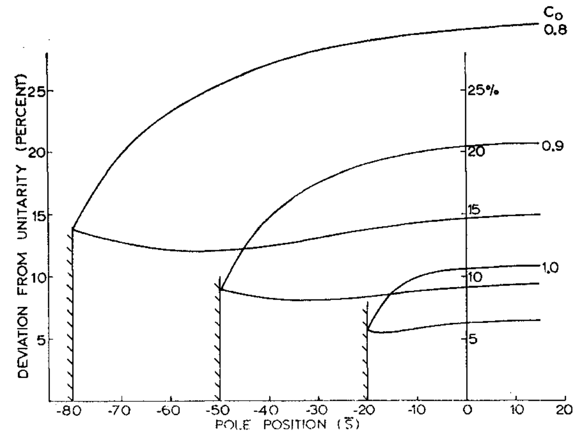

FIG. 10. Variation of the rms deviation from unitarity with position of the short-range pole in the $T=\frac{3}{2}$ π–N s-wave calculation for different values of the parameter C_0, the parameter C_1 being fixed at $C_1=-0.95$.

(56)] are consistent with the absolute minimum of $\Delta(C_0,C_1)$ for the $T=\frac{3}{2}$ case. In Fig. 11, we show the phase shift α_3 which is given by $\mathrm{Re}F'(s)=(\sin 2\alpha_3)/2q$ for $C_0=1.025$, $C_1=-0.94$. The agreement between this phase shift and the input data is good. Therefore, the results in the $T=\frac{3}{2}$ case are consistent with the results in the $T=\frac{1}{2}$ case.

VIII. SOLUTION FOR THE $(\frac{3}{2},\frac{3}{2})$ π–N RESONANCE

We now show how the variational method can be used to predict the position and width of the $(\frac{3}{2},\frac{3}{2})$ π–N resonance. The weight function $\rho(s)$ which appears in Eqs. (18) is calculated for the short Born cut $(M-\mu^2/M)^2\leq s\leq M^2+2\mu^2$, the crossed cut $0\leq s\leq (M-\mu)^2$, and the arc $0\leq|\arg s|\leq 66°$ of the circle $|s|=M^2-\mu^2$ (Fig. 2), in the manner indicated in parts (i), (ii), and (iii) of Sec. VI. The remainder of the weight function is represented by a short-range pole, as in Eq. (49).

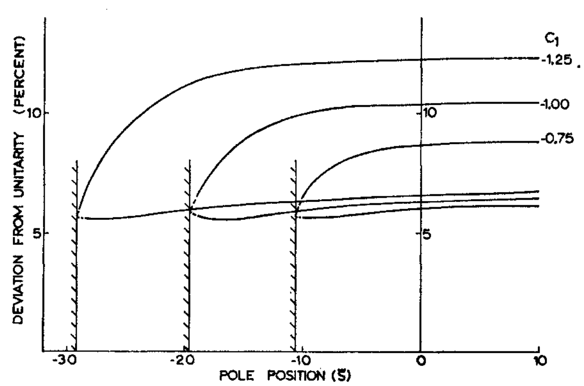

FIG. 9. Variation of the rms deviation from unitarity with position of the short-range pole in the $T=\frac{3}{2}$ π–N s-wave calculation for different values of the parameter C_1, the parameter C_0 being fixed at $C_0=1.00$.

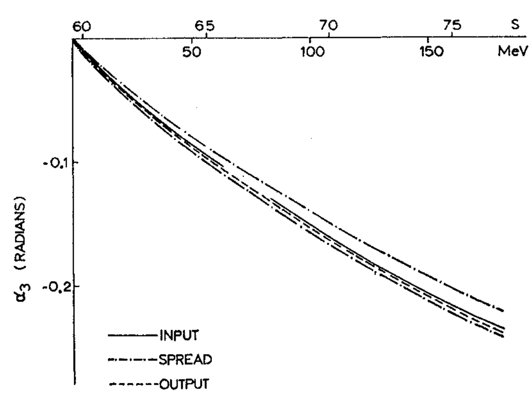

FIG. 11. Comparison of the input value with the $T=\frac{3}{2}\pi$–N s-wave phase shift α_3 and error spread obtained, using the values obtained in the $T=\frac{1}{2}\pi$–N s-wave calculation for the parameters C_0 and C_1.

We make a few comments on the various parts of $\rho(s)$. The short Born cut gives a strong long-range attraction[24]; this dominates the low-energy scattering. The value of $\rho(s)$ on the crossed cut $0<s\leq(M-\mu)^2$ is small. The main reason for this is the factor (1/9) which occurs in the p-wave crossing matrix. The $T=1$ $J=1$ $\pi-\pi$ contribution to the front of the circle ($0\leq|\arg s|\leq 66°$) is also small in the $(\frac{3}{2},\frac{3}{2})$ case. It is calculated in the same way as discussed for the $T=\frac{1}{2}$ case in Sec. VII. We use the coupling constant $C_1=-0.94$.

The $T=0$ $J=0$ π-π contribution is also calculated in the same way as discussed for the $T=\frac{1}{2}$ case in Sec. VII. This corresponds to a $T=0$ $J=0$ π-π scattering amplitude having parameters $\nu_1=-30, \Gamma=15$ in the notation of HMOV[16] (it gives the $T=0$ s-wave π-π scattering length $a_0=1.3$). Also we use $C_0=1.0$ [cf. Eq. (50)]. The $T=0$ $J=0$ π-π contribution to the $(\frac{3}{2},\frac{3}{2})$ amplitude gives an attraction which is about a quarter the size of the long-range Born term, and is also of fairly long range.[16]

The present calculation is certainly not from first principles. However, there appears to be a good prospect of carrying out a calculation from a more fundamental standpoint. This depends on the fact that the $T=1$ $J=1$ π-π term and the crossed-cut term are small, and the $T=0$ $J=0$ π-π term is only about one-quarter of the long-range Born term. Starting from the long-range Born term alone, it should be possible to get an approximation to the $(\frac{3}{2},\frac{3}{2})$ resonance, using the variational method. Feeding this result back, and assuming that we know the $T=0$ $J=0$ π-π scattering amplitude, we could get an approximation to the $T=0$ $J=0$ $\pi+\pi\to N+\bar{N}$ contribution from the front of the circle. Also, we could similarly approximate the contribution from the cut $0\leq s\leq(M-\mu)^2$. Now, iteration should give the result.[26]

For the present, however, we shall calculate the $(\frac{3}{2},\frac{3}{2})$ resonance, using the values of the weight function $\rho(s)$ determined in the way that we discussed above, plus the arbitrary short-range pole [Eq. (49)].

Method of Calculation

The amplitude

$$F(s)=f_{1+}^{(3/2)}(s)/q^2$$

[Eq. (14)] is used. Various unitary trial functions $F_p(s)$ are inserted in Eqs. (18). These trial functions have parameters (a_i), and we vary (a_i) and the short-range pole parameters $\bar{s}, \Gamma$ to make $F'(s)$ as close to unitarity as possible. The method is very similar to that described in Sec. VII for the $T=\frac{1}{2}$ case.

The residue Γ is determined, for given $\bar{s}$ and (a_i), by the unitary condition

$$\{\mathrm{Re}F'(s'')\}^2+\{\mathrm{Im}F'(s'')\}^2=\mathrm{Im}F'(s'')/\{q(s'')\}^3, \quad (57)$$

using $s''=68$ (i.e., 87.5-MeV lab pion energy). We now evaluate $D_p(s)$ and Δ_p [Eqs. (20a) and (20b)]. It turns out that one of the roots Γ_i gives a much better fit to unitarity (i.e., much smaller Δ_p) than the other root. The latter root is rejected. Next, $\bar{s}$ is varied from the origin along the negative real axis to get the minimum value of Δ_p. This determines $\bar{s}$ and Γ for the parameter values (a_i). Let $\Delta(a_i)$ be the corresponding value of Δ_p. Now, the parameters (a_i) are varied to obtain the absolute minimum of $\Delta(a_i)$. This gives the solution $F'(s)$, which can then be verified by consistency (cf. Sec. IV above).

Threshold Behavior

Near the threshold $s_0=(M+\mu)^2$, unitarity requires that the p-wave amplitude obey

$$\mathrm{Im}F(s)=0(q^3) \quad \text{as} \quad q\to 0. \quad (58)$$

This means that the right-hand side of the second of Eqs. (18) should vanish at $s=s_0$. We have fitted unitarity exactly at $s=s''$ by Eq. (57), and condition (58) will not, in general, be obeyed by our solution $F'(s)$. To satisfy Eq. (58), it would be necessary to add a second short-range pole. This would make the calculation rather complicated and has not been done. In fact, a small error in $\mathrm{Im}F'(s)$ near $s=s_0$ will have little effect on the resonance.

We modify the unitary fitting so as to exclude the threshold s_0. In Eq. (20b) for Δ_p, we replace s_0 ($=59.6$) by $s_0'=62.0$. In practice, this is quite satisfactory. As Δ_p is reduced by variation, the deviation from unitarity near the threshold is found to reduce rapidly.

Breit-Wigner Solution I

In searching for a resonant solution, the simplest trial function to use is

$$F_p(s)=\gamma/(\omega_R-\omega-i\gamma q^3), \quad (59)$$

where $\omega=(1+q^2)^{1/2}$, q being the momentum in the c.m. system. The real parameters ω_R and γ give the position and width of the resonance. We use the form (59) from threshold up to 450 MeV. Above 2 BeV, we use

$$\mathrm{Im}F_p(s)=1/2q^3, \quad \mathrm{Re}F_p(s)=0. \quad (60)$$

This corresponds to a completely absorptive partial wave at high energies. In Sec. VI, we gave arguments for believing that such high-energy conditions will be an effective substitute for our lack of knowledge of the short-range interaction. This means that, however many parameters (a_i) are introduced into the trial function $F_p(s)$, we expect to get a unique solution $F'(s)$. Actually, as will be seen below, if the number of parameters (a_i) is *small*, the best solution $F'(s)$ is determined by very different conditions, and the exact form of the high-energy behavior Eq. (60) is unimportant.

[26] The $T=1$ $J=1$ π-π term could be ignored in the $(\frac{3}{2},\frac{3}{2})$ case with little error.

In the energy region 450 MeV to 2 BeV, smooth forms of $\text{Re}F_p(s)$ and $\text{Im}F_p(s)$ are used to join on smoothly to Eqs. (59) and (60). These forms in the intermediate energy region will vary as ω_R and γ are varied. It will be seen below that the precise shape of $\text{Re}F_p(s)$ and $\text{Im}F_p(s)$ in the intermediate region has little effect on our results.

The parameters ω_R and γ are varied over the range $1.5\leq\omega_R\leq 2.5$, $0.05\leq\gamma\leq 0.25$. The range for ω_R corresponds to a lab pion kinetic-energy range of 110 to 320 MeV. It is more convenient in the calculations to use the corresponding range of values[27] of s. We have $s_R=[(M^2+\omega_R^2-1)^{1/2}+\omega_R]^2$ and the range is $70\leq s_R\leq 90$.

Having determined the short-range pole parameters $\bar{s}$, Γ for given values of ω_R and γ, as described above, we obtain $\Delta(\omega_R,\gamma)$ which is the root-mean-square deviation from unitarity for these values of ω_R and γ. The contour plot of $\Delta(\omega_R,\gamma)$ is shown in Fig. 12. The absolute minimum value of $\Delta(\omega_R,\gamma)$ is 16% and it occurs for $\gamma=0.176$, $s_R=77.6$ (i.e., lab pion kinetic energy 187 MeV). The deviation from unitarity is so large that we do not expect a good solution. This is borne out by the consistency test, as can be seen in Fig. 13. There, we show the real parts of the input $F_p(s)$ for $\gamma=0.176$, $s_R=77.6$, the output $F'(s)$ and the experimental values[28] $F(s)$. All three curves differ noticeably, and we conclude that the simple Breit-Wigner form [Eq. (59)] is not a suitable trial function.

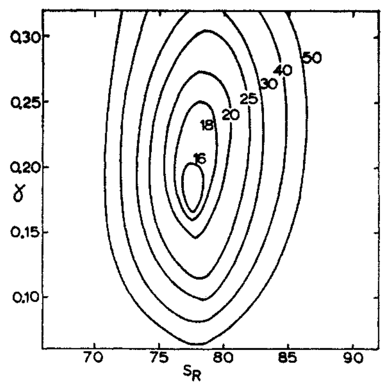

FIG. 12. Contour plot of the rms deviation from unitarity $[\Delta(s_R,\gamma)]$ as a function of the resonance position s_R and width γ for the Breit-Wigner approximation in the $(\frac{3}{2},\frac{3}{2})$ π–N resonance calculation.

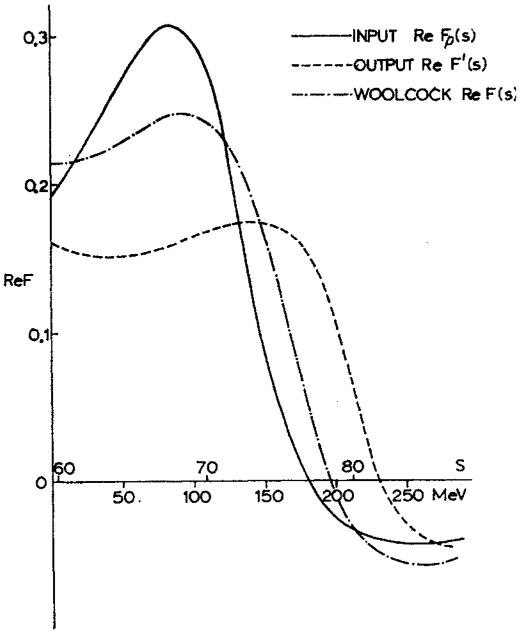

FIG. 13. Comparison of the input, output, and experimental (Ref. 18) real parts of the $(\frac{3}{2},\frac{3}{2})$ p-wave π–N amplitude in the Breit-Wigner approximation.

Breit-Wigner Solution II

It was shown in Sec. V that, when the trial function $F_p(s)$ gives a poor approximation, the results can be improved by using the function

$$G'(s)=\tfrac{1}{2}[F_p(s)+F'(s)]$$

in place of $F'(s)$. This improvement occurs because $G'(s)$ has the correct singularities on the physical sheet, whereas the physical-sheet singularities of $F'(s)$ which lie to the left of the threshold $s_0=(M+\mu)^2$ may be badly wrong.

We use the same form for $F_p(s)$ as in the section immediately preceding [i.e., Eqs. (59) and (60) etc.]. Δ_p is now defined by replacing $F'(s)$ in Eqs. (20) by $G'(s)$, and the analysis proceeds as before. The contours of $\Delta(\omega_R,\gamma)$ are shown in Fig. 14. The absolute minimum of $\Delta(\omega_R,\gamma)$ is now less than 6% and occurs for $\gamma=0.192$, $s_R=75.0$ (i.e., 160-MeV lab energy). In Fig. 15, it is seen that the output function $G'(s)$ is fairly close to the experimental values, although the corresponding input $F_p(s)$ is noticeably different. Obviously, using $G'(s)$ makes a considerable improvement.

In Fig. 14, there is another minimum of $\Delta(\omega_R,\gamma)$ somewhere near the bottom of the diagram ($\gamma<0.10$).

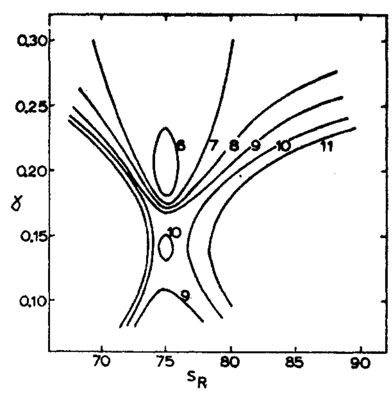

FIG. 14. Contour plot of the percentage rms deviation from unitarity $[\Delta(s_R,\gamma)]$ as a function of the resonance position s_R and width γ for the improved Breit-Wigner approximation in the $(\frac{3}{2},\frac{3}{2})$ $\pi-N$ resonance calculation.

[27] The relation between s and the lab pion total energy ω_L is (with $\mu=1$) $s=M^2+1+2M\omega_L$ ($M=6.7$).

[28] The experimental values are the values due to Woolcock [see W. S. Woolcock, Ph.D. thesis, University of Cambridge, 1961, and J. Hamilton and W. S. Woolcock, Rev. Mod. Phys. 35, 737 (1963)].

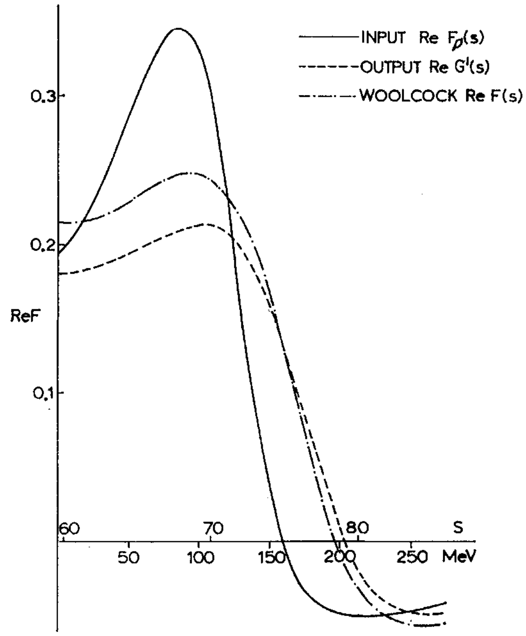

FIG. 15. Comparison of the input, output, and experimental (Ref. 18) real parts of the $(\frac{3}{2},\frac{3}{2})$ p-wave π–N amplitude in the improved Breit-Wigner approximation.

This corresponds to a spurious solution, and it can be rejected by checking whether the corresponding $G'(s)$ satisfies the dispersion relation (i.e., the consistency check). Such spurious solutions are apt to occur if we use a trial function $F_p(s)$ which does not reduce Δ_p to values very much below 10%.

Layson Method

Clearly, we must use a trial function which is more sophisticated than the simple Breit-Wigner form, if we are to get a good approximation to unitarity. A formula which Layson[29] suggested as an empirical fit to the experimental values of the α_{33} phase shifts turns out to be very satisfactory for our purpose. It is

$$F_p(s)=\gamma_1/(\omega_R-\omega-i\gamma_1 q^3) \tag{61a}$$

where

$$\gamma_1=\frac{2M\gamma_L}{\omega+\omega_R}\cdot\frac{a^3}{1+(qa)^2}. \tag{61b}$$

Here, ω_R, γ_L, and a are positive parameters. We use Eqs. (61) from threshold up to 450 MeV, and then join on smoothly to the values in Eq. (60) which are used above 2 BeV (this joining is done in the same way as for the Breit-Wigner case).

In the Breit-Wigner form, the centrifugal barrier-penetration effect is described by the factor $q^{2l+1}=q^3$ in the denominator. In Layson's form, this is replaced by the factor

$$\frac{(qa)^3}{1+(qa)^2}\cdot\frac{1}{\omega+\omega_R}.$$

Even in a relativistic process this should be a considerable improvement, since a high-energy particle does not have to penetrate such an extensive potential barrier. The parameter a will be of the order of the range of the interaction. Layson obtained a good fit[29] to the experimental data, using $\omega_R=1.973$ (i.e., $s_R=79.3$, corresponding to 205 MeV), $\gamma_L=0.133$, $a=0.714$ (units $\hbar=\mu=c=1$).

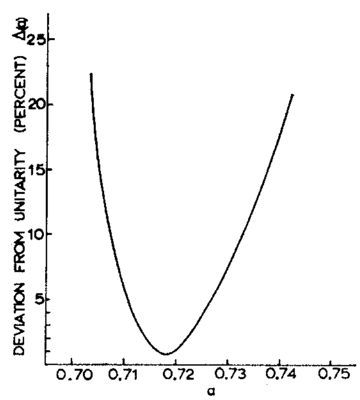

FIG. 16. Variation of the rms deviation from unitarity as a function of the parameter a for the Layson approximation in the $(\frac{3}{2},\frac{3}{2})$ π–N resonance calculation.

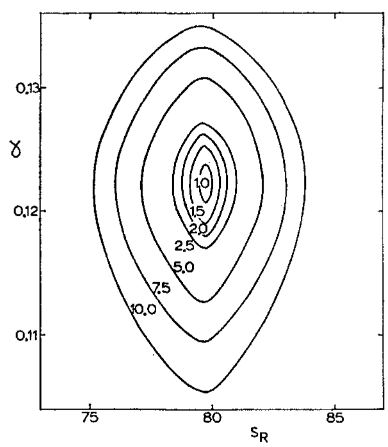

FIG. 17. Contour plot of the percentage rms deviation from unitarity $[\Delta(s_R,\gamma_L,a)]$ as a function of the resonance position s_R and the reduced width γ_L, with the parameter a fixed at its best value $a=0.718$, for the Layson approximation in the $(\frac{3}{2},\frac{3}{2})$ π–N resonance calculation.

The trial function $F_p(s)$ is substituted in Eq. (18), and the root-mean-square deviation from unitarity Δ_p is defined in terms of $F'(s)$ by Eqs. (20a) and (20b). The parameters are varied over the ranges $70\leq s_R\leq 90$, $0.10\leq\gamma_L\leq 0.15$, $0.65\leq a\leq 0.75$. For given values of s_R, γ_L, a, the parameters $\bar{s}$, Γ of the short-range pole are determined in the way that we described for Breit-Wigner solution I.

For each value of a, the contours of the unitary deviation $\Delta(s_R,\gamma_L,a)$ are plotted in the plane of s_R and γ_L, and the minimum value $\Delta(a)$ is determined. As a is varied, these minimum values $\Delta(a)$ are found to lie on a curve which itself has a minimum at $a=0.718$ (Fig.

[29] W. M. Layson, Nuovo Cimento **20**, 1207 (1961); CERN preprint, 1961 (unpublished).

16). Figure 17 shows the contours of $\Delta(s_R,\gamma_L,a)$ for $a=0.718$. From this, we find that the absolute minimum of Δ is 0.8% and occurs at $s_R=79.4$, $\gamma_L=0.124$, $a=0.718$. This is a good fit to unitarity. Also, the sections of $\Delta(s_R,\gamma_L,a)$ through the minimum point rise steeply, so the values of the parameters can be determined accurately.

Our solution gives the resonance at 206 MeV, and the width at half-height is 120 MeV. In Fig. 18, we show the real parts of the input function $F_p(s)$ corresponding to the absolute minimum of Δ, the output or solution $F'(s)$, and the experimental values[28] $F(s)$. Obviously, the self-consistency of the solution is good. Further, the solution $F'(s)$ agrees with the experimental values to within the experimental errors, or a little

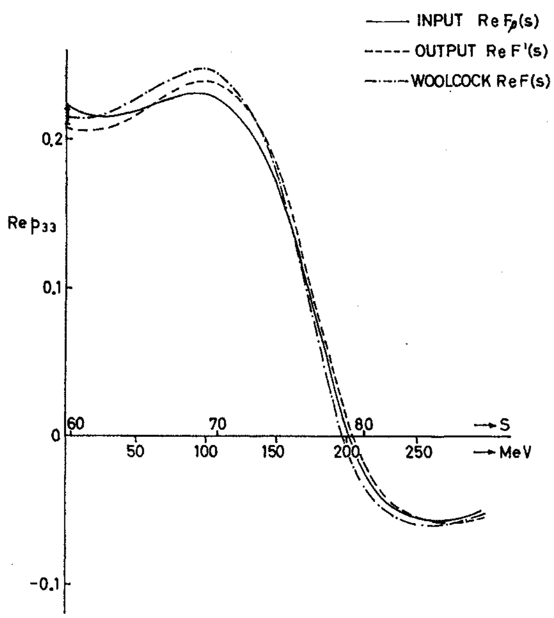

FIG. 18. Comparison of the input, output, and experimental (Ref. 18) real parts of the $(\frac{3}{2},\frac{3}{2})$ p-wave π–N amplitude in the Layson approximation.

more. As we would expect from the arguments in Sec. V, the function $G(s)=\frac{1}{2}\{F_p(s)+F'(s)\}$ gives even better agreement with the experimental values.

The short-range pole associated with our solution $F'(s)$ lies at $\bar{s}=-120$, so it is well to the left of the circle. Its residue Γ is small, and the short-range contribution to Re$F'(s)$ at threshold is -0.003.

Crossing of the Real Part

We have not used the fact that the real part of the $(\frac{3}{2},\frac{3}{2})$ partial wave $F(s)$ has to satisfy crossing symmetry, so that its value on the crossed cut $0\leq s\leq(M-\mu)^2$ is related to its value on the physical cut $(M+\mu)^2\leq s\leq\infty$. This provides an *independent* check on our calculation of the short-range pole.

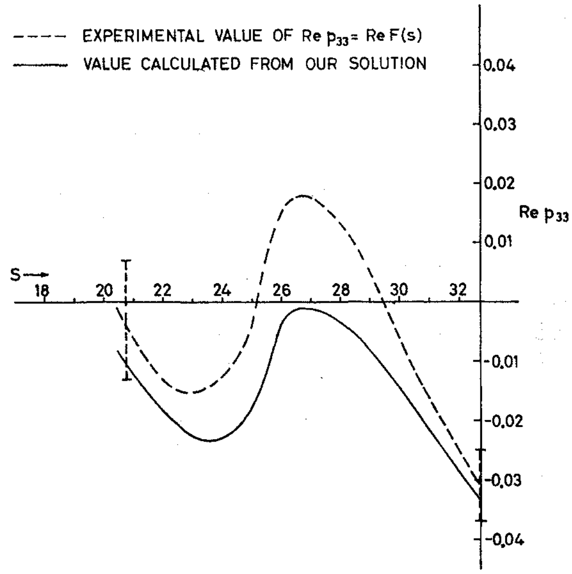

FIG. 19. Comparison of the output and experimental (Ref. 18) real parts of the $(\frac{3}{2},\frac{3}{2})$ p-wave π–N amplitude on the crossed cut for the Layson approximation.

This check is made by calculating the real part of the amplitude on $20\leq s\leq 32.7=(M-\mu)^2$ (cf. Fig. 2) in two ways:

(i) We use the first of Eqs. (18) to evaluate Re$F'(s)$ on the crossed cut. For $F_p(s)$, which appears in the physical integral, we use the Layson form as defined above [Eqs. (61) and (60)] with the best values of the parameters (i.e., $s_R=79.4$, $\gamma_L=0.124$, $a=0.718$). The values of $\rho(s)$ on the short Born cut, the cut $0\leq s\leq(M-\mu)^2$, and the arc $0\leq|\arg s|\leq 66°$ of the circle are those described at the beginning of Sec. VIII. For the short-range pole [Eq. (49)], we use the values of the parameters $\bar{s}$, Γ which were determined above. Now, a simple calculation gives Re$F'(s)$ as shown in Fig. 19.

(ii) Re$F(s)$ for $20\leq s\leq 32.7$ is evaluated in terms of the physical values of the low-energy $\pi-N$ partial-wave amplitudes by crossing.[30] Only the s-wave and p-wave $\pi-N$ amplitudes need be considered, since d-wave corrections to Re$F(s)$ are small, except for $s\lesssim 20$. In Fig. 19, we show the values of Re$F(s)$ obtained by using the experimental s-wave and p-wave π–N data.[20] Two further facts have to be noted: (a) the $(\frac{3}{2},\frac{3}{2})$ amplitude Re$F(s)$ itself $\{(M+\mu)^2\leq s\leq 90\}$ gives the major contribution to Re$F(s)$ on the crossed cut $(20\leq s\leq 32.7)$; (b) by Fig. 18, we see that Re$F(s)\simeq$Re$F'(s)$ where $F'(s)$ is our solution.

Thus, by comparing the calculations in (i) and (ii), we are checking our solution Re$F'(s)$ *with itself* by crossing. It is seen from Fig. 19 that the agreement with crossing is reasonably satisfactory.[31] The reason why

[30] See Refs. 2 and 5 for the details of this calculation.

[31] The slight difference in the shape of the two curves in Fig. 19 can be attributed to the difficulty of obtaining an accurate evaluation of the principal-value integral over the crossed cut which was used in computing Eq. (18) for $s<32.7$.

crossing of the real part provides a good check on the short-range pole can be understood by a simple example. Suppose that the pole lies far to the left (i.e., $\bar{s}$ is large and negative). Increasing the residue Γ by $\delta\Gamma$ will, to a first approximation, increase $\text{Re}F'(s)$ [Eq. (18)] by[32] $\delta\Gamma/(s_0-\bar{s})$, *both* on the crossed cut *and* on the low-energy part of the physical cut. However, there is a factor (1/9) in the crossing matrix which relates the $(\frac{3}{2},\frac{3}{2})$ amplitude on the crossed cut to its physical values.

At the beginning of Sec. VIII, we remarked on the prospects of carrying out a calculation from a more fundamental standpoint, in which only the low-energy $T=0$ $J=0$ and $T=1$ $J=1$ π–π phase shifts and f^2 are given. Such a calculation would have to involve both s-wave and p-wave π–N amplitudes, and it seems likely that the device of crossing the real part would then play an important role in finding the solution.

IX. DISCUSSION OF THE $(\frac{3}{2},\frac{3}{2})$ RESONANCE SOLUTION

We now examine several general points in connection with our $(\frac{3}{2},\frac{3}{2})$ solution which was derived from the Layson formula Eq. (61).

Variation Solutions having Only a Few Parameters

If we use a sufficient number of parameters (a_i) in the trial function $F_p(s)$, our solution $F'(s)$ should become increasingly accurate. At the same time, difficulties arise because we do not know the spectral function $\rho(s)$ [Eq. (18)] over the whole of the left-hand cuts. As was pointed out in Sec. VI, there is good reason to believe that we can avoid these difficulties by: (a) *assuming* that the far-away singularities can be represented by a simple pole $\Gamma/(s-\bar{s})$; (b) determining the parameters $\bar{s}, \Gamma$ of this pole by imposing high-energy boundary conditions, such as

$$\text{Im}F(s)\to 1/2q^3,\quad \text{Re}F(s)=0(1/q^4),\quad \text{as}\quad q\to\infty$$

on our solution $F(s)$.

However, in the Breit-Wigner and Layson solutions which were given in Sec. VIII, there are only two and three parameters, respectively. This means that we are far from the situation which has just been discussed for the case of many parameters. Several points arise:

(i) The real test that we have obtained approximately the correct short-range effect for low physical values of s is the check by crossing $\text{Re}F(s)$, as discussed at the end of Sec. VIII.

(ii) We might have assumed a different form for the trial function $F_p(s)$ in the intermediate energy region (450 MeV to 2 BeV). In fact, it is easy to verify that considerable deviations from the form that we used in the intermediate region only make a small change in the short-range pole and make hardly any change in the parameters of the $(\frac{3}{2},\frac{3}{2})$ resonance.[33]

(iii) We might enquire why our method of calculating the short-range effect in the case of the two- or three-parameter trial function happens to give such a good result, since our method appears at first sight to be in contradiction with the N/D method. We shall examine this point in a little more detail.

Relation to the N/D Method

The N/D method automatically gives a unitary partial-wave amplitude $F(s)$. We assume that the long-range part of the spectral function $\rho(s)$ is given. Then, the short-range part of $\rho(s)$ can be chosen arbitrarily, and by varying this part it would appear that we could alter $F(s)$ in an arbitrary manner.

We now give a simple example which shows that there are cases in which the long-range part of the spectral function dominates the low-energy scattering, irrespective of the value of the short-range part (with one exceptional value). Let $F(s)$ be a p-wave amplitude whose cuts are $-\infty\leq s\leq s_1$ and $s_0\leq s\leq\infty$. The momentum is given by $q^2=s-s_0$. The N/D equations are

$$F(s)=N(s)/D(s);\tag{62a}$$

$$N(s)=\frac{1}{\pi}\int_{-\infty}^{s_1}\frac{D(s')\rho(s')}{s'-s}ds';\tag{62b}$$

$$D(s)=D(s_0)-\frac{s-s_0}{\pi}\int_{s_0}^{\infty}\frac{N(s')q'^3}{(s'-s_0)(s'-s)}ds'.\tag{62c}$$

Now, we choose the spectral function

$$\rho(s)=-\pi\Gamma_B\delta(s-s_B)-\pi\Gamma_F\delta(s-s_F).\tag{63}$$

If $(s_0-s_B)/(s_0-s_F)\ll 1$, we have clearly separated long-range (B) and short-range (F) parts of $\rho(s)$. Substituting Eq. (63) in Eq. (62b) gives

$$N(s)=\frac{\Gamma_BD_B}{s-s_B}+\frac{\Gamma_FD_F}{s-s_F},\tag{64}$$

where we write $D_B\equiv D(s_B)$, $D_F\equiv D(s_F)$. Substituting Eq. (64) in Eq. (62) and integrating gives, for $s>s_0$,

$$D(s)=D(s_0)-\frac{(s-s_0)}{(s-s_B)}a_B\Gamma_BD_B-\frac{(s-s_0)}{(s-s_F)}a_F\Gamma_FD_F -iq^3\left\{\frac{\Gamma_BD_B}{s-s_B}+\frac{\Gamma_FD_F}{s-s_F}\right\},\tag{65a}$$

[32] As usual, $s_0=(M+\mu)^2$.

[33] The effect of inserting another resonance in $F_p(s)$ at 850 MeV is to alter the short-range contribution at threshold by about 0.002, but otherwise there is little change in the low-energy solution.

and, for $s<s_0$,

$$D(s)=D(s_0)-\frac{(s-s_0)}{(s-s_B)}a_B\Gamma_B D_B-\frac{(s-s_0)}{(s-s_F)}a_F\Gamma_F D_F - (s_0-s)^{3/2}\left\{\frac{\Gamma_B D_B}{s-s_B}+\frac{\Gamma_F D_F}{s-s_F}\right\}. \quad (65b)$$

Here, $a_B=(s_0-s_B)^{1/2}$, $a_F=(s_0-s_F)^{1/2}$, and all square roots take the positive value.

Letting $s\to s_B$ Eq. (65) gives

$$D_B=D(s_0)+\tfrac{1}{2}\Gamma_B D_B a_B+\Gamma_F D_F\frac{a_B^2}{a_F+a_B}. \quad (66a)$$

Similarly,

$$D_F=D(s_0)+\Gamma_B D_B\frac{a_F^2}{a_F+a_B}+\tfrac{1}{2}\Gamma_F D_F a_F. \quad (66b)$$

Solving Eqs. (66), we get

$$D_B=\frac{D(s_0)}{\Delta}\left\{1+\Gamma_F\left[\frac{a_B^2}{a_B+a_F}-\tfrac{1}{2}a_F\right]\right\},$$
$$D_F=\frac{D(s_0)}{\Delta}\left\{1+\Gamma_B\left[\frac{a_F^2}{a_B+a_F}-\tfrac{1}{2}a_B\right]\right\}, \quad (67)$$

where

$$\Delta=1-\tfrac{1}{2}(\Gamma_B a_B+\Gamma_F a_F)+\tfrac{1}{4}\Gamma_B\Gamma_F a_B a_F\left\{\frac{a_F-a_B}{a_F+a_B}\right\}^2.$$

Now, we use the fact that $a_B\ll a_F$. Then,

$$\Delta\simeq(1-\tfrac{1}{2}\Gamma_B a_B)(1-\tfrac{1}{2}\Gamma_F a_F);$$

$$D_B\simeq\frac{D(s_0)}{1-\frac{1}{2}\Gamma_B a_B},\quad D_F\simeq\frac{D(s_0)(1+\Gamma_B a_F)}{(1-\frac{1}{2}\Gamma_B a_B)(1-\frac{1}{2}\Gamma_F a_F)}. \quad (68)$$

We evaluate

$$\mathrm{Re}\left\{\frac{1}{F(s)}\right\}=\mathrm{Re}D(s)/N(s)$$

for $s>s_0$, using Eqs. (64) and (65a) for $\mathrm{Re}D(s)$ and $N(s)$. We make one further approximation. Where the term $1/(s-s_F)$ appears in Eqs. (64) and (65a), we replace it by $1/(s_0-s_F)=a_F^{-2}$. This is good enough for a low-energy approximation.

We get

$$\mathrm{Re}\left\{\frac{1}{F(s)}\right\}\simeq\frac{1-\frac{3}{2}\Gamma_B a_B+\dfrac{a_B^3\Gamma_B}{s-s_B}}{\dfrac{\Gamma_B}{s-s_B}+\dfrac{\Gamma_F}{a_F^2}\dfrac{1+\Gamma_B a_F}{1-\frac{1}{2}\Gamma_F a_F}}. \quad (69)$$

Except for the case that $1-\frac{1}{2}\Gamma_F a_F\simeq 0$, the second term in the denominator is small as compared with the first term at low energies. We now neglect the second term in the denominator, noting that this approximation is particularly good if Γ_F has a large positive or negative value. This gives

$$\mathrm{Re}\left\{\frac{1}{F(s)}\right\}\simeq\frac{1}{\Gamma_B}\{(s-s_B)(1-\tfrac{3}{2}\Gamma_B a_B)+a_B^2\Gamma_B\}. \quad (70)$$

Clearly we would also obtain Eq. (70) if we had started with $\Gamma_F=0$.

Thus, apart from the case that $1-\frac{1}{2}\Gamma_F a_F=0$, the low-energy scattering is almost independent of the short-range part of the interaction [by low energies, we mean values of s such that $(s-s_B)\ll\frac{1}{2}(s-s_F)$]. Equation (69) shows that this approximation is particularly good in the neighborhood of a resonance (which occurs if $\Gamma_B>2/3a_B$).

In the exceptional case, $1-\frac{1}{2}\Gamma_F a_F\simeq 0$, Eq. (68) shows that $|D_F/D_B|$ becomes large. By Eq. (64), we see that this means that we tend to get scattering which is dominated by the short-range part of the interaction. When that happens, the scattering amplitude will vary very slowly with energy in the physical region.

CONCLUSION

This example suggests that, while it is not possible to determine the short-range part of the spectral function from low-energy scattering (cf. Castillejo *et al.*[11]), there are cases in which the variational method with a few parameters will be accurate. In such cases, the long-range interactions dominate low-energy scattering, so the scattering amplitude at low energies can be adequately described by a few poles on the physical and unphysical sheets. Then, a fairly simple trial function $F_p(s)$ containing only a few parameters will give a good approximation. This appears to be the situation for the $(\frac{3}{2},\frac{3}{2})$ amplitude.[34]

Finally, we emphasize again that crossing of the real part of the amplitude is the ultimate check on the validity of our $(\frac{3}{2},\frac{3}{2})$ solution.

ACKNOWLEDGMENTS

One of us (AD) is indebted to the Department of Scientific and Industrial Research for the award of a Research Fellowship. He would also like to thank the National Institute for Research in Nuclear Science for their hospitality and use of computing facilities.

[34] Because we use the amplitude $F(s)=f_{1+}^{(3/2)}/q^2$, and because $q^2\to\infty$ as $s\to\pm0$ (Fig. 2), we would not expect the short-range pole to lie much to the right of the point $s=-(M^2-\mu^2)=-44$. Thus, the short-range and long-range parts of $\rho(s)$ are well-separated in the p-wave π-N case.